Aus der

Universitätsklinik für Urologie

The expression of CD276 (B7-H3) on different urothelial carcinoma cell lines in comparison to somatic urothelial cells

Inaugural-Dissertation

zur Erlangung des Doktorgrades

der Medizin

der Medizinischen Fakultät

der Eberhard-Karls-Universität

zu Tübingen

vorgelegt von

Maurer, Florian Basilius

2022

Dekan:	Professor Dr. B. Pichler
1. Berichterstatter:	Professor Dr. W. K. Aicher
2. Berichterstatter:	Professor Dr. G. Klein
Tag der Disputation:	04.08.2022

Table of Contents

For reasons of the legibility, the male form was chosen in this thesis. However, if not specified otherwise, this text refers to all genders.

List of Abbreviations

APS	Ammonium Persulfate
AUA	American Urological Association
BC	Bladder Cancer
BCG	Bacillus Calmette-Guérin
CD	Cluster of Differentiation
cDNA	Complementary deoxyribonucleic acid
DEPC	Diethylpyrocarbonate
DNA	Deoxyribonucleic acid
DPBS	Dulbecco's phosphate-buffered saline
DR	Duplication rate
EAU	Euopean Association of Urology
EDTA	Ethylenediaminetetraacetic acid
EMT	Epithelial-Mesenchymal-Transition
GAPDH	Glyceraldehyde 3-phosphate dehydrogenase
HRP	Horseradish Peroxidase
Ig	Immunoglobulines
KCS	Keratinocyte Standart
kDa	Kilo Dalton
MEM	Minimum Essential Medium
MIBC	Muscle-invasive Bladder Cancer

MMC	Mitomycin C
NMIBC	Non-muscle-invasive Bladder Cancer
PBD	Pyrrolobenzodiazepine
PBS	Phosphate buffered saline
PPIA	Peptidylprolyl isomerase A
qRT-PCR	Real-time quantitative reverse transcription polymerase chain reaction
RIPA	Radioimmunoprecipitation assay
RISC	RNA-induced silencing complex
RNA	Ribonucleic acid
SDS-PAGE	Sodium dodecylsulfate polyacrylamide gel electrophoresis
TAG	Transgelin
TEMED	Tetramethylethylendiamine
TREM	Triggering receptor expressed on myeloid cells
Tris	Tris(hydroxymethyl)aminomethane
TURB	Transurethral resection of the bladder
UC/UCC	Urothelial carcinoma, Urothelial carcinoma cell, Urothelial cell carcinoma
UTR	Untranslated region
WHO	World Health Organisation

List of Figures

List of Tables

1 Introduction

1.1 Clinical and pathological Features of Urinary Bladder Cancer

The incidence and mortality of cancer are rapidly growing worldwide. It is expected to become the major cause of death in the 21st century (Bray et al., 2018). With an incidence of 549,000, cancer of the urinary bladder ranks as the 10th most common form of cancer worldwide, resulting in approximately 200,000 deaths annually (Bray et al., 2018). However, there is a significant difference in incidence and mortality by geographical region and sex (Antoni et al., 2017). The incidence of bladder cancer (BC) is highest in North America, Europe and parts of Western Asia, while mortality rates are higher in developing countries (Cumberbatch et al., 2018). Men have higher rates of incidence and mortality with 9.6 and 3.2 per 100,000, respectively. It is about 4 times those of women worldwide. As in most cancers, the incidence increases with age (Bray et al., 2018) and the majority of BC is diagnosed at age >65 (Sanli et al., 2017).

Risk factors for developing urinary BC can be sorted into external exposures and internal factors (Burger et al., 2013). By far the most common external risk factor is tobacco smoking, as tobacco contains several carcinogenic aromatic amines and polycyclic aromatic hydrocarbons. Tobacco smoking is believed to be responsible for 50% of BC cases (Burger et al., 2013). Smoking cessation may reduce the risk for developing BC, as former smokers have lower incidences than active smokers (Gabriel et al., 2012). Because e-cigarettes contain similar carcinogenic chemicals, they potentially present a risk factor comparable to tobacco smoking (Fuller et al., 2018). Occupations with exposures to carcinogens presents another potent risk factor for developing BC. Workers in the production industry of aluminum, rubber and dye have a higher

risk of developing BC. Occupations in the coal-tar pitch industry, as hairdressers or barbers, in the printing industry or as textile manufacturers present suspected risk factors (Cumberbatch et al., 2018). Dietary factors may also present risk factors for BC. Obese and overweight patients with non-muscle-invasive BC (NMIBC) had a higher rate of recurrence when compared to patients with normal weight (Westhoff et al., 2018). Other risk factors for BC include medical preconditions such as previous radiotherapy treatment of prostate cancer (Abern et al., 2013), schistosomiasis infections, white race, low socioeconomical status and treatment with certain drugs (Cumberbatch et al., 2018). Internal risk factors are mainly genetic alterations with patients having a background of BC in their family (Burger et al., 2013).

The vast majority of BC, between 90% to 95%, are urothelial carcinomas (UCs). 5% to 10% are adenocarcinomas, squamous cell carcinomas or tumors of other types (Reuter, 2006). Morphologically, BC can present as papillary, solid or mixed type. At the time of diagnosis, 3/4 of patients have NMIBC and 1/4 have muscle-invasive BC (MIBC) (Kamat et al., 2016). BC can be further differentiated into high-grade and low-grade carcinomas. Half of NMIBCs are low grade, while the majority of MIBCs and metastatic tumors are high grade (Humphrey et al., 2016). In NMIBC, tumors are described as low, intermediate or high risk tumors (Sylvester et al., 2006). For invasive tumors, the classification follows the grading G1-G3 of the WHO-Classification of 1973 (van de Putte et al., 2018). As urothelial carcinomas frequently present as multifocal tumors, each tumor has to be analyzed individually concerning tumor type and clone origin (Catto et al., 2006). One of the proposed pathogenesis pathways for urothelial tumors is via genetic alterations in the *FGFR3* gene, which activates the *RAS/MEK/ERK*-pathway (Billerey et al., 2001). Furthermore, the immune system of the body with its pro- and anti-inflammatory effects plays a major role in the development of this disease (Thompson et al., 2015).

The most common symptom patients with urothelial BC experience, is painless hematuria. 10-20% of patients with macroscopic hematuria have tumors of the bladder (Bruyninckx et al., 2003). Cystoscopy, urine cytology, sonography and CT or MRI screening are methods for diagnosing bladder cancer (Sanli et al., 2017). A suitable urinary marker with a higher sensitivity than cystoscopy is yet to be found (Schmitz-Dräger et al., 2015). BC is classified according to the TNM classification of 2016 displayed in Figure 1 and staged from 0a to IV (S3-Leitlinie Harnblasenkarzinom, 2016).

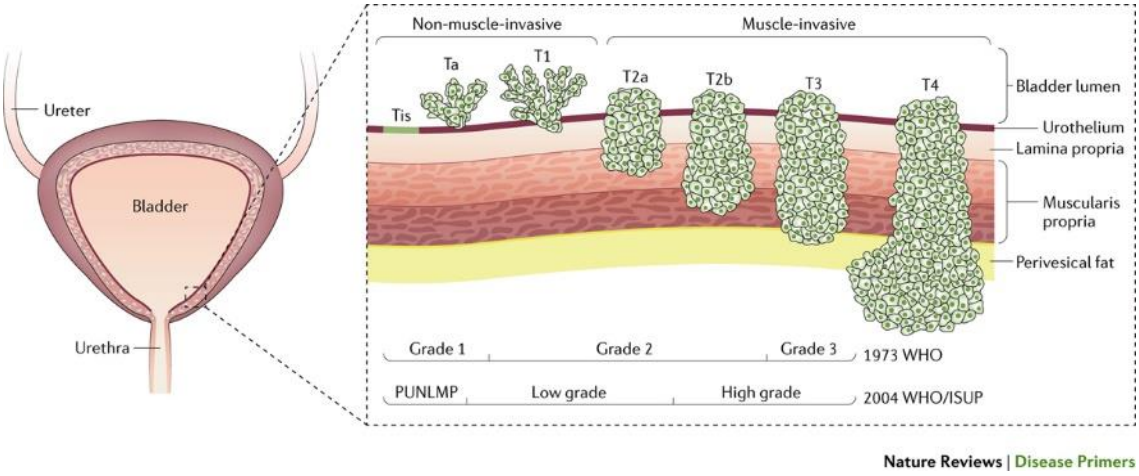

Figure 1: Staging of bladder cancer according to Tumor, Node, Metastasis (TNM) system of 2016. Histological classification of 1973 by the WHO and of 2004 by WHO/ISUP are shown. PUNLMP: papillary urothelial malignancy of low malignant potential.
From :Sanli, O. *et al.* (2017) Bladder cancer
Nat. Rev. Dis. Primers doi:10.1038/nrdp.2017.22

Treatment of urothelial bladder cancer depends on many factors including stage and grade of the tumor, as well as invasiveness. Generally, NMIBCs are treated with transurethral resection of the bladder (TURB) and optional intravesical installation of agents such as mitomycin C (MMC) or Bacillus Calmette-Guérin (BCG) (Rayn et al., 2018). In case of failure of BCG-Installation, the European Association of Urology (EAU) and the American Urological Association (AUA) recommend radical cystectomy (Chang et al., 2016), (S3-Leitlinie Harnblasenkarzinom, 2016). For MIBC, radical cystectomy in combination with bilateral pelvine lymphadenectomy is the standard treatment with curative intention for the patient (Shariat et al., 2006). A platinum based (neo-)adjuvant chemotherapy is generally recommended for patients ≥cT2 and increases the

overall survival by 5-10% after 10 years (Vale, 2005). The standard first-line therapy of the metastasized stage IV urothelial bladder cancer is a cisplatin-based combination therapy. For a second line therapy, immune therapies are of increasing importance and several studies have proven the effectiveness of PD1- and PD-L1- Inhibitors (Bellmunt et al., 2017, Sharma et al., 2017, Powles et al., 2017).

1.2 CD276 (B7-H3) and its Significance in Tumors

In 2001, Chapoval et al. described a new molecule of the B7 superfamily of immune checkpoint molecules, designated B7-H3 or CD276. In humans, it is encoded on chromosome 15 (Chapoval et al., 2001). It is a type I membrane protein, has a molecular weight of approximately 110 kDa and consists of four Ig-like domains: An IgV-like and an IgC-like domain, which are duplicated (Steinberger et al., 2004). The molecule exists in a membrane-bound, as well as soluble form (Xie et al., 2016). CD276 is ubiquitously expressed in many tissues on a low level suggesting a strictly regulated posttranscriptional mechanism, which is further discussed in 1.3 (Nygren et al., 2011, Janakiram et al., 2017). It was shown to have a higher expression in many types of cancer, including squamous cell carcinoma, gastric cancer, ovarian cancer, pancreatic cancer, prostate cancer, liver cancer, glioma, melanoma- and bladder cancer and was associated with invasive potential and proliferation in different tumors. An association with worse outcome and prognosis was also seen (Dong et al., 2018, Xylinas et al., 2014, Zhou et al., 2013, Wang et al., 2013). Furthermore, CD276 overexpression in urothelial cell carcinoma of the bladder indicated a significantly shorter overall survival of patients and was associated with a poorer prognosis (Xu et al., 2018). Conversely, high expression of CD276 was associated with a better survival for patients with gastric and pancreatic cancer in two studies (Loos et al., 2009, Wu et al., 2006). The discrepancy may be explained by a different methodology used, the time point of CD276 measurement or different cancer subtypes (Dong et al., 2018).

Currently, the receptor for CD276 has not yet been identified on human samples. In 2012, Hashiguchi et al. demonstrate specific binding of *TLT2* from the *TREM* receptor family to CD276. However, other studies were not able to validate these results and did not observe a direct interaction between *TREM* receptors and CD276 (Leitner et al., 2009, Li et al., 2018a). Overexpression of B7 family molecules in the vicinity of tumors has been linked to reduction of anti-tumor immunity and immune evasion of the tumor (Leung and Suh, 2014). For CD276, several functions have been established. Many of its functions may help to establish tumor progression and lead to the development of “Hallmarks of cancer” (Hanahan and Weinberg, 2011). First of all, it is believed to act as a co-stimulatory, as well as a co-inhibitory factor in the anti-tumor response of the immune system (Li et al., 2018a).

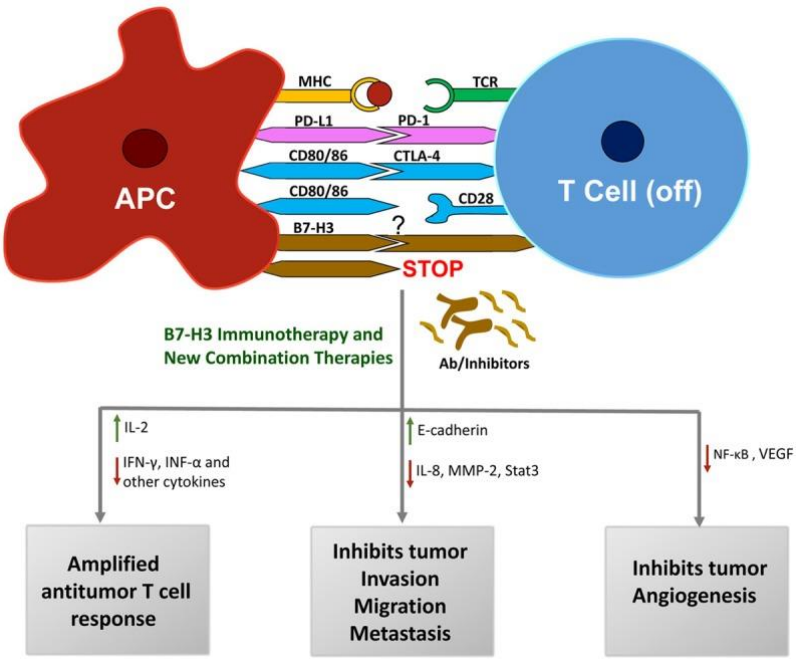

Figure 2: Antigen-presenting cell (APC) interacting with a T-Cell. Display of different immune checkpoint molecules with their respective receptors inducing an inhibitory response on the immune system. Possible therapeutic effects of B7-H3 inhibition by antibodies (Ab).
From :Jose R Castellanos, et al. Am J Clin Exp Immunol. 2017;6(4):66-75.

Furthermore, CD276 is not only believed to influence the tumor immunity and evasion, but also to play a role in the tumor invasion, migration and metastasis as shown in Figure 2 (Castellanos et al., 2017). It may be able to promote epithelial-mesenchymal-transition (EMT) in cancer by decreasing E-cadherin expression (Jiang et al., 2016b). The proposed molecular pathway inducing migration and invasion in bladder cancer cells is facilitated *via* the *PI3K/Akt/STAT3* pathway, which also mediates resistance to a variety of chemotherapeutics in different cancers (Li et al., 2017, Zhang et al., 2017, Jiang

et al., 2016a). Another “Hallmark of cancer”, the Warburg effect, was observed to be stimulated by CD276 (Lim et al., 2016). It is characterized by a shift from aerobic to anaerobic metabolism in (tumor) cells even in the presence of sufficient oxygen (Vander Heiden et al., 2009).

Targeting CD276 in anti-tumor therapy is in its early stages but has shown promsing results so far. Several clinical trials have proven the effectivness of immunotherapy *in vivo* against CTLA-4 and B7 family member PD-1 with its ligand to reverse inhibitory signaling on T-Cells by tumor cells in different cancers (Phan et al., 2003, Iwai et al., 2002). Similar results could be expected for anti-CD276 immunotherapy with multiple clinical trials, currently in Phase I or Phase II, underway. *Enoblituzumab* is a monocolonal antibody targeting CD276. Multiple clinical trials alone or in combination with other immune checkpoint targeting antibodies indicate promising antitumor effects with no dose-limiting toxicity or severe immune related side effects (Flem-Karlsen et al., 2018, Powderly et al., 2015). An Fc-engineered monoclonal antibody developed by Loo et al. was able to inhibit the growth of renal cell carcinoma and bladder carcinoma tumor xenografts *in vivo.* Another therapeutic approach presents the monoclonal antibody *m276* equipped with a Pyrrolobenzodiazepine (PBD) warhead. It was shown to kill both cancer cells and tumor vasculature overexpressing CD276 in different tumor models in mice. Few side effects and significant regression of the tumor was observed (Seaman et al., 2017). It may present another promising strategy for targeting CD276.

Limitations to therapies with antibodies include variable tissue penetration, heterogeneous distribution in solid tumors, different routes of application and, most importantly, resistance of the tumor to antibody therapy (Chames et al., 2009).

1.3 MicroRNAs and their regulatory Role for CD276 Expression

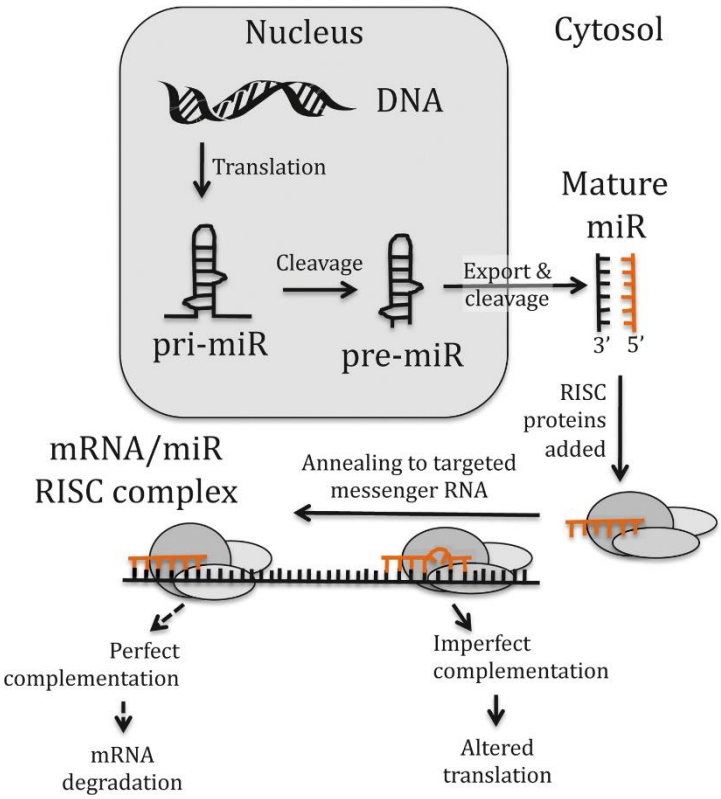

Figure 3: Illustration of microRNA (miRNA) synthesis and the mechanism of messenger RNA (mRNA) regulation. RISC=RNA-induced silencing complex. From: *Catto et. al, 2011 MicroRNA in Prostate, Bladder, and Kidney Cancer: A Systematic Review. European Urology, 59, 671-681.*

Around 98% of the transcriptional output of humans was found to consist of non-protein coding RNAs (Shruti et al., 2011, Mattick, 2001). MicroRNAs or miRNAs are a specific group of these non-coding RNAs with a length of around 22 nucleotides, which play a major role in post-transcriptional regulation of genes (Ambros, 2004). They were first discovered in 1993 and are single-stranded RNA molecules built by an RNase-III-type enzyme from an endogenous transcript that contains a local hairpin structure (Kim, 2005, Lee et al., 1993, Shruti et al., 2011). The antisense strands (guide strands) of these RNA molecules are built into RNA-induced silencing complexes (RISCs), which contain enzymes, Dicer and other cellular factors (Rana, 2007). By complementary base pairing with mRNA molecules, RICSs facilitate cleavage of these mRNA molecules, destabilization of mRNA molecules or inhibition of translation into proteins in ribosomes (Fabian et al., 2010, Bartel, 2009). An overview of this process is shown in Figure 3. It is important to note that miRNAs may have multiple target mRNAs with varying effects on expression.

The link between miRNA and the growth of cancer was first discovered in chronic lymphocytic leukemia patients having a down-regulation of *miR-15a* and *miR-16-1* (Calin et al., 2002). In cancer, miRNAs may function as oncogenes (*oncomiRs*) or tumor suppressor genes, depending on their target structure (Hammond, 2006). In the case of CD276, multiple miRNAs interfering post-transcriptionally with the expression of the gene have been found or are suspected in various cancers. In breast cancer, nearly 50 miRNAs have been identified, which downregulate CD276 protein levels. Furthermore, 13 of these were found to directly bind to the 3'-UTR region. Most notably, the expression of *miRNA 29c* correlates with survival in breast cancer patients, suggesting a tumor suppressive role for this miRNA (Nygren et al., 2014). In bladder cancer, downregulation of *miRNA 29c* in established UCC cell line T24 and bladder cancer tissue was observed (Fan et al., 2014). Moreover, *miRNA 29c* interactions lead to decreased CD276 protein levels in cancers such as neuroblastoma, sarcoma and melanoma (Wang et al., 2013, Xu et al., 2009). In colorectal cancer, *miRNA 187* inhibits cell proliferation, migration and invasion by directly binding CD276 mRNA and suppressing its expression (Wang et al., 2016). A lower expression of *miRNA 187* was also found in high-risk ovarian cancer patients, possibly acting as a tumor suppressor (Dong et al., 2018). Numerous other miRNAs interacting with CD276 mRNA on a post-transcriptional level have been identified (Nygren et al., 2014).

There is a significant therapeutic potential of miRNAs, as restoration of normal expression levels in cancer could be able to target multiple genes and pathways simultaneously (Pereira et al., 2013). MiRNAs could also serve as clinical biomarkers, even if a regulatory function of a specific miRNA is not observed (Farazi et al., 2011). Furthermore, detection and analysis of miRNAs in urine may be a useful non-invasive tool in diagnosing urothelial cell carcinoma (Mengual et al., 2013).

1.4 Aim of this Work

The pathologic role of CD276 (B7-H3) has already been established in different types of cancer. In UC, the relationship between CD276 and immune evading mechanisms, as well as the invasive and migrative potential of the tumor has also been described. Studies indicate a higher expression of CD276 mRNA, as well as CD276 protein inside and outside the tumor cell in correlation with poor prognosis and decreased overall survival of patients.

This leads to the assumption that dysregulation of CD276 may be an important factor in development and progression of UC.

It was also shown that miRNAs may play a major role in regulation of CD276 mRNA expression. Especially *miRNA 29c* could function as a tumor suppressor by decreasing CD276 mRNA levels in tumor cells.

The aim of this work is to confirm the hypothesis of dysregulated CD276 expression in selected and established urothelial carcinoma cell (UCC) lines. Expression of CD276 at the level of transcription into mRNA, translation into protein and presentation at the cell surface is to be analyzed and compared to somatic urothelial cells. Correlation of this data may show, to what extend the amounts of expression are in relationship with each other.

Furthermore, miRNA expression in cell lines with high, moderate and low expression of CD276 protein are analyzed to confirm a possible regulatory role. To the best of my knowledge, expression of miRNAs in established urothelial carcinoma cell lines has only been tested in cell line *T24*. Results may also help understanding the complex function of miRNAs in the progress and tumorigenesis of urothelial carcinoma.

2 Material and Methods

2.1 Devices and Equipment

Table 1: Devices used with Name and Manufacturer

Device	Name	Manufacturer
Blot Scanner	C-DiGit® Blot Scanner	LI-COR
Centrifuge	CombiSpin FVL-2400N	bioSan
Centrifuge	Centrifuge 5424	eppendorf
Centrifuge	3-30KS	Sigma
Centrifuge	Rotina 420R	Hettich
Centrifuge	Heraeus Multifuge 3SR+	ThermoFisher Scientific
Clean Bench	SL-1200	BDK
Electrical pipetting device	Pipetus	Hirschmann Laborgeräte
ELISA Reader	Kinetic Analyzer	Milenia DPC
FACS Device	BD LSR II	BD-Biosciences
Incubator	Heracell 240i	ThermoFisher Scientific
Lens-10x	Primo-Plan-ACHROMAT 10x/0,25 Ph1 415500-1605-001	Zeiss
Lens-20x	Primo-Plan-ACHROMAT 20x/0,30 Ph1 415500-1614	Zeiss
Lens-40x	Primo-Plan-ACHROMAT LD-40x/0,5 Ph2 415500-1616	Zeiss
Microscope	Primovert	Zeiss
pH Meter	pH Level1	inoLab
Photospectrometer	NP80 Mobile	Implen

Pipette 0,5-10µl; 10-100µl; 20-200µl; 100-1000µl	Eppendorf research	eppendorf
Pipette 0,5-10µl; 10-100µl; 20-200µl; 100-1000µl	Eppendorf reference	eppendorf
Scale	440-47N	Kern
Shaker	DSG 304/M4	Heidolph
Stirrer with Agitator	MR82	Heidolph
Vacuum pump	mini-pump	KNF
Thermoblock	UNO II	Biometra
Thermoblock	LightCycler 480 II	Roche
Thermomixer	Thermomixer comfort	eppendorf
Voltage Generator	PowerPack P25	Heidolph
Vortex Decive	MS1 Minishaker	IKA
Waterbath	1083	GFL

Table 2: Consumables, Reference Number and Manufacturer

Consumable	Reference Number	Manufacturer
96-well plate F-Bottom	655 180	Greiner bio-one
96-well plate for Light Cyler	04729692001	Roche
96-well plate U-Bottom	650 180	Greiner bio-one
Advantage RT-for-PCR-Kit	639506	Takara
DC Protein Assay Kit II	5000112	Sigma
Disposable Scalpel No.10	02.001.30.010	Feather
Cryogenic storage tube	368632	ThermoScientific
Disposable bags	759705	Brand
FACS-Tubes	352052	Falcon

Gloves-Nitril, powder-free M	290419	ABENA
Micro test tube 0,5 ml	0030 121.023	Eppendorf
Micro test tube 1,5 ml	616 201	Greiner bio-one
Micro test tube 2 ml	0030 120.094	Eppendorf
Bath stabilizer	1-6095	neoLab
Parafilm	P 7543	Sigma-Aldrich
Pasteur Pipettes	200760	WU Mainz
Petri dish	101VR20	Thermo Scientific
RNA Mini Kit	74106	Quiagen
Cell scraper	3010	Corning
Cell culture flask blue vented cap	353136	Falcon
Cell culture flask Cellbind Surface	T25: 3289; T75: 3290	Corning
Centrifugation tubes	15 ml: 188217; 50ml: 227261	Greiner bio-one

2.2 Reagents and Solutions

Table 3: Reagents

Reagents	Reference Number	Manufacturer
30% Acrylamid-Mix	161-0156	BioRad
Accutase	A6964-100ML	Sigma
Advantage RT-for-PCR-Kit	639506	Takara
Agarose	9012-36-6	Sigma-Aldrich
Ampuwa	7151-5	Fresenius
Aprotinin	9087-70-1	Sigma-Aldrich

Bovine Serum Albumin (BSA) 25%	A10008-01	Gibco
CD276 Primer	Forward Sequence: TTTCCTTTCCCCTCCTTCCTCC Reverse Sequence: TGTGACCAGCACATGCTTCC	Eurofins
Cholera Toxin 1mg	100B	Biological Laboratories Inc.
DC Protein Assay Kit II	5000112	BioRad
DMSO	D2650-5X5ML	Sigma
Dulbeccos Phosphate Buffered Saline (DPBS)	D8537-500ml	Sigma
EDTA Versen (1% w/v)	L2113	Biochrom
Ethanol absolute	20821.330	VWR Chemicals
FCS	26140079	Gibco
FSL-1	SML1420-100UG	Sigma
GAPDH Primer	Forward Sequence: GAGTCAACGGATTTGGTCGT Reverse Sequence: TTGATTTTGGAGGGATCTCG	Biomol GmbH
Gel Red Nucleic Acid Gel stain 10000x in water	41003	Biotinum
Gentamycin 10mg/ml	A 2712	Biochrom
HEPES Buffer Solution (1M)	15630-056	Gibco
Keratinocyte standard medium	37000-015	Gibco
LightCycler 480 SybrGreen I Master	04887352001	Roche
MEM Earle’s	FG0325	Biochrom
Mercaptoethanol	A338,0100	AppliChem
Methanol 100%	20847.307	VWR Chemicals
Milk powder		Tip
miR-148b-3p PCR Primer	YP00204047	Qiagen
miR-181b-5p PCR Primer	YP00204530	Qiagen
miR-187-3p PCR Primer	YP00201018	Qiagen
miR-187-5p PCR Primer	YP00205920	Qiagen
miR-29a-3p PCR Primer	YP00204698	Qiagen
miR-29a-5p PCR Primer	YP00204430	Qiagen

miR-29c-3p PCR Primer	YP00204729	Qiagen
miR-29c-5p PCR Primer	YP00204135	Qiagen
miR-524-3p PCR Primer	YP00204030	Qiagen
miR-524-5p PCR Primer	YP00204135	Qiagen
miR-539-5p PCR Primer	YP00205656	Qiagen
miR-874-3p PCR Primer	YP00204761	Qiagen
miRCURY LNA miRNA PCR Assay	339306	Qiagen
miRNeasy Mini Kit	217004	Qiagen
MycoSPY Mykoplasma detection kit	M030-050	Biontex
Non-essential amino acids	11140-035	Gibco
PBS-drops (WesternBlot)	18912-014	Gibco
Penicillin/Streptomycin	15140-122	Gibco
PPIA Primer	Forward Sequence: TTCATCTGCACTGCCAAGAC Reverse Sequence: TCGAGTTGTCCACAGTCAGC	Biomol GmbH
RIPA-Buffer + PMSF 200mM	PL-25-M	CC Pro
RNA Mini Kit	74106	Quiagen
RNase free DNase Set	79254	Quiagen
RNeasy MinElute Cleanup Kit	74204	Qiagen
SDS 10% (w/v) Solution	1610416	BioRad
SNORD49a PCR Primer	YP00203904	Qiagen
Sodium Pyruvat 100mM	11360-039	gibco
Tetramethylethylendiamin (TEMED)	2367	Roth
Tris-Glycine Buffer	161-0734	BioRad
Trypan blue 0,4%	17-942E	Lonza
Trypsin	12563-011	Gibco
Tween20	9005-64-5	Fisher
WesternBlot secondary AB rabbit-anti-mouse HRP	P0260	Dako
WesternBlot-AB Anti-b-Actin	ab8227	abcam

Westernblot-AB Anti-CD276	ab105922	abcam
WesternSure Premium Chemiluminescent Substrate:	926-95000	LI-COR

Table 4: Mediums and Solutions

Medium/Solution	Constituents/Properties
Urothelial Cell Growth Medium	KCS Medium, 1% CT, 1% Pen/Strep
Urothelial Carcinoma Cell Growth Medium	MEM Earle's Medium, 10% FCS, 1% NEA, 1% Pen/Strep
Freezing Medium	50% KCS/MEM Earle's Medium, 40% FCS, 10% DMSO
Tissue Transportation Medium	0,35 g/l $NaHCO_3$, 1% 10mM HEPES, 0,26% 20 KIU/ml Aprotinin, 1% Pen/Strep
Tissue Stripping Solution	HBSS 0,35 g/l $NaHCO_3$, 1% 10mM HEPES, 0,26% 20 KIU/ml Aprotinin, 1% Pen/Strep, 10% of 1% (w/v) EDTA solution
Membrane Stripping Solution	dist. H_2O 95% (v/v), 0,2 M Glycine 1,5% (w/v), 0,1%SDS 0,1% (w/v), 1%Tween20 0,5% (v/v); pH 2,2
PFEA buffer	2% FCS, 0,02% Sodium azide, 97,8% DPBS 74% (w/v) EDTA

2.3 Urothelial Carcinoma and Somatic Cell Lines

Table 5: Cell Lines used for analysis of CD276 expression with their corresponding reference

Cell Line	Reference	Classification
UM-UC-5	Grossman et al. (1986)	Tumor: Bladder Cancer Tumor Stage (TNM): unknown Patient: female, Age: unknown
UM-UC-6	Grossman et al. (1986)	Tumor: Bladder Cancer Tumor Stage (TNM): unknown Patient: male, Age unknown
UM-UC-9	Shinohara et al. (1993)	Tumor: Bladder Cancer Tumor Stage (TNM): unknown Patient: unknown
UM-UC-10	Sabichi et al. (2006)	Tumor: Bladder Cancer Tumor Stage (TNM): unknown Patient: unknown
UM-UC-13	Sabichi et al. (2006)	Tumor: Lymphatic metastasis of Bladder Cancer Tumor Stage (TNM): unknown Patient: unknown
UM-UC-14	Sabichi et al. (2006)	Tumor: Renal pelvis tumor Tumor Stage (TNM): unknown Patient: unknown
UM-UC-15	Park et al. (2008)	Tumor: Bladder Cancer Tumor Stage (TNM): unknown Patient: unknown
UM-UC-16	Sabichi et al. (2006)	Tumor: Bladder Cancer Tumor Stage (TNM): unknown Patient: unknown

Table 6: Cell Lines used for analysis of miRNA expression with their corresponding reference

Cell Line	Reference	Classification
TCC sup.	Nayak et al. (1977)	Tumor: Bladder Cancer Tumor Stage (TNM): TxNxM1 Patient: female, Age 67
5637	Fogh et al. (1977)	Tumor: Bladder Cancer Tumor Stage (TNM): unknown Patient: male, Age 68
Cal-29	Cattan et al. (2001)	Tumor: Bladder Cancer Tumor Stage (TNM): T2NxM1 Patient: female, Age 80
HT1197	Rasheed et al., (1977)	Tumor: Bladder Cancer Tumor Stage (TNM): TxNxM1 Patient: male, Age 44
253J	Elliott et al., (1974)	Tumor: Retroperitoneal lymphatic node metastasis Tumor Stage (TNM): TxNxM1 Patient: male, Age 53
UM-UC-16	Sabichi et al. (2006)	Tumor: Bladder Cancer Tumor Stage (TNM): unknown Patient: unknown
UM-UC-6	Grossman et al. (1986)	Tumor: Bladder Cancer Tumor Stage (TNM): unknown Patient: male, Age unknown

The UCC lines shown in Table 6 were chosen according to their level of CD276 protein expression relative to somatic urothelium. *UC 6* and *UC 16* were chosen as cell lines expressing low relative amounts of CD276 protein, as shown in chapter 3.3. *TCC* and *253J* with low-to-medium amounts of CD276 protein. *Cal-29* and *5637* with medium-to-high protein expression and *HT1197* with high relative CD276 protein expression (values from unpublished results by research groups of Prof. Dr. Aicher). Different levels of protein expression were thought to be outlining best a possible correlation between miRNA expression and CD276 protein expression.

This work was approved by the Ethics Committee of the University of Tübingen Hospital (UKT) and the Eberhard-Karls-University Tübingen under File Number 279/2013 B02.

2.4 Tissue Processing and Extraction of Somatic Cells

Bladder or ureter tissue was extracted from patients clinically free of tumors and immediately placed in sterile tubes filled with transportation medium (Table 4). It was then stored at 4°C or directly transported on ice for further processing. The tissue was then placed in a sterile petri dish containing 5 ml Keratinocyte Standard (KCS) medium. Residues of adipose tissue or vessels were removed and the tissue was cut into 1-2 cm^2 pieces. Those pieces were transferred into 15 ml of stripping solution specified in Table 4 and incubated for 3 hours at 37°C and 5% CO_2. Subsequently, the piece of tissue was placed in 3 ml KCS medium and scraped off with a cell scraper. The tissue was again rinsed with medium and the material was collected in a 15 ml centrifugation tube. Upon centrifugation at 200 g for 5 minutes with a brake of 1-2, the supernatant was removed and the pellet suspended in 2,5 ml KCS medium. Subsequently, it was transferred to a T25 CellBIND culture flask and cultured at 37°C and 5%CO_2. AE1/AE3 staining was applied for proof of somatic urothelial origin. AE1/AE3 generally stains positive in carcinomas of epithelial origin by staining certain cytokeratines. It is used to distinguish between somatic and carcinoma cells.

2.5 Cell Cultivation and Harvesting

For long term storage, the urothelial carcinoma (UC) cell lines mentioned in 2.3 were suspended in freezing medium (Table 4). For short term storage, the tubes were stored at -80°C. Somatic urothelial cells were stored in a different freezing medium (Table 4), respectively. For thawing, the cryogenic tubes were placed in a 37°C water bath until almost completely unfrozen. The contents were then transferred into 20 ml of KCS medium for urothelial cells or 10 ml of Minimum Essential Medium (MEM) for UCCs. This was followed by centrifugation for 5 minutes at 200g and a brake of 1-2. The cell pellet was

suspended in 20 ml KCS medium for urothelial cells and 10 ml MEM medium for UCCs. Finally, the suspension was transferred to a T75 CellBind culture flask, which was placed in an incubator at 37°C and 5% CO_2 for cultivation. Every 2-3 days the growth medium was removed from the flasks and new growth medium was added (Table 4). Cells were harvested at around 80% Confluence. 4 ml of 0,1 % ethylenediaminetetraacetic acid (EDTA) solution were added to the cell culture for breakdown of cell-to-cell adhesion. After 8 minutes of incubation at 37°C and 5%CO_2, the 0,1 % EDTA solution was removed and 1,5 ml TrypLE™ Select was added and incubated for 1-2 minutes. Cell loosening was observed under the microscope. 10 ml of medium were added, suspended with contents of the flask and then transferred to a centrifugation tube. The centrifuge was run at 200 g for 5 min with a brake of 1-2. The pellet was processed further, depending on the intention of the experiment.

2.6 Passaging and Duplication Rate

When cell culture flasks reached around 80% confluent, cells had to be passaged to a new cell culture flask. They were released from the surface of the flask and processed as described in chapter 2.5. The cell pellet was then resuspended with 10 ml of medium. At this point, a cell count was performed using a Neubauer cell counting chamber using trypan blue dye exclusion. 20 µl of trypan blue were mixed with 20 µl of the resuspended medium containing the cells. The cell counting chamber was filled with the suspension. All four quadrants were counted and an average cell count was obtained. Viable cells remain clear while dead cells appear dark blue. The number was corrected for the 1:1 dilution and the cell number was calculated. The measure the duplication rate of each individual cell line, cell numbers of a culture were obtained at the point of seeding and at the point of harvesting.

$$DR = \frac{\left(\frac{\log_{10}\left(\frac{N1}{N2}\right)}{\log_{10}(2)}\right)}{d}$$

Duplication Rate per 24 hours;
N1= Number of cells at point of seeding;
N2= Number of cells at point of harvest;
d= Number of days between seeding and harvest;
(Bieback et al., 2004)

The duplication rate (DR) was calculated with the above-mentioned equation.

2.7 Quantification of the CD276 mRNA Transcription with qRT-PCR

2.7.1 RNA Extraction

The level of transcription for the messenger ribonucleic acid (mRNA) of the CD276 gene was determined using real-time quantitative reverse transcription polymerase chain reaction (qRT-PCR). Each cell line was cultured and processed to obtain a cell pellet as described in chapter 2.5. The cells were then washed with 10 ml of approximately 4°C cold PBS and subsequently centrifuged at 200 g for 7 minutes with a brake of 1-2. The supernatant was removed and a cell pellet remained. To extract the mRNA from the cells, the cell pellet was suspended in 350 µl RLT-Buffer containing 1% β-mercapthoethanol and subsequently stored at -70°C for at least 24 hours. Upon thawing, 350 µl of a 70% ethanol solution were added, the solution was mixed in a syringe and then transferred to a spin column. Next, the columns were centrifuged at 9400 g for 15 seconds. The flow-through was discarded and 350 µl RW1 washing buffer were added. A centrifugation step at 9400 g for 15 seconds followed and the flow-through was discarded. 80 µl of DNase solution were added to the column (Table 4), which was then incubated for 15 minutes at room temperature. After the incubation, 350 µl of RW1 buffer were added and the column was centrifuged at 9400 g for 15 seconds. The column was placed in a

new collection tube, 500 µl of RPE buffer were added and the column was centrifuged at 9400 g for 15 seconds. Again, the flow-through was discarded. Subsequently, 500 µl of RPE buffer were added, the column was centrifuged at 9400 g for 2 minutes and the flow-through was discarded. The column was then centrifuged at 9400 g for 15 seconds to dry the membrane. Finally, the column was placed in a new tube, 40 µl of RNase-free-water were added and a centrifugation step at 9400 g for 1 minute followed. The tube containing the RNA was sealed and stored at -80°C until reverse transcription.

2.7.2 Reverse Transcription of RNA into cDNA

The reagents for the reverse transcription were stored at -20°C and were vortexed, shortly centrifuged and put on ice upon thawing. The samples from 2.7.1 were immediately put on ice after thawing. The ribonucleic acid (RNA) concentrations in the samples were determined and, in a new tube, a volume containing 1 µl of RNA was filled up to a volume of 12,5 µl with diethylpyrocarbonate (DEPC)-treated water. 1 µl of oligo dT-primer was added to each sample. Subsequently, the samples were transferred to a PCR cycler and heated for 2 minutes at 70°C. Next, 6,5 µl of a master-mix were prepared and added to each sample (Table 7). The samples were placed in the PCR block and incubated for 60 minutes at 42°C. Immediately after, the samples were heated to 94°C and incubated for 5 minutes. Finally, 80 µl of DEPC-treated water were added to each sample containing the complementary deoxyribonucleic acid (cDNA) and the samples were stored at -20°C.

Table 7: Composition of master-mix for transcription of RNA to cDNA per sample

Reagent	Volume
5xbuffer	4 µl
RNase inhibitor	0,5 µl
dNTP-Mix	1 µl
reverse transcriptase	1 µl

2.7.3 CD276 qRT-PCR

The qRT-PCR trials were carried out with a LightCycler® 480 System. SYBR Green was used as a fluorescence dye. As reference genes for the target gene CD276, peptidylprolyl isomerase A (PPIA) and glyceraldehyde 3-phosphate dehydrogenase (GAPDH) were used. In a 96-well-plate, 2 µl cDNA template was placed in each well. From the samples produced in 2.7.2, six wells were filled with template and for every gene, two measurements were taken. 18 µl of a master-mix prepared according to Table 8 and containing the appropriate primer was added to each well.

Table 8: Composition of master-mix for CD276 qRT-PCR per well

Reagent	Volume
SYBR Green	10 µl
Primer	2 µl
Non-template water	6 µl

A negative control was obtained by adding non-template water in a well and adding 18 µl of the master-mix mentioned in Table 8, respectively. A technical positive control was obtained by targeting the transgelin (TAG) gene in cDNA obtained from smooth muscle cells. A schematic layout for preparation of the 96-well plate is shown in Figure 4. After preparation of the 96-well plate, it was covered with a transparent film and centrifuged at 235 g for 1 minute. The efficiencies of the primers used were as follows:

Table 9: Primer efficiencies for CD276 qRT-PCR

Gene	**Melting temperature (°C)**	**Primer efficiency**
CD276	60	1,775
GAPDH	60	1,66
PPIA	60	1,787

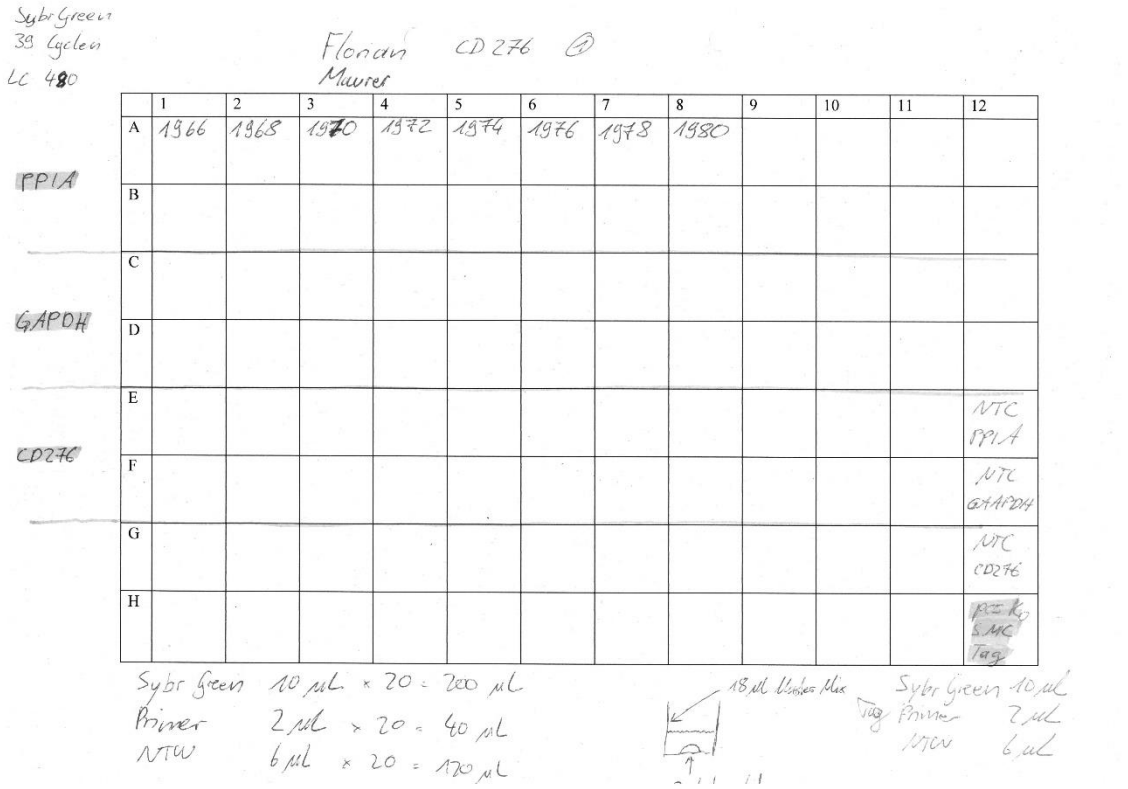

Figure 4: Schematic layout of the 96-well plate for the CD276 qRT-PCR

The qRT-PCR was run according to features in Table 10 for 39 cycles at 60°C. Figure 5 shows a schematic illustration of the amplification cycles run in the qRT-PCR. Figure 6 illustrates the melting curves of the samples in the qRT-PCR.

Table 10: Features of CD276 qRT-PCR with temperature and time

Program	Temperature	Time	Cycles
Denaturation	95°C	5 minutes	1
Amplification	95° - 60° - 72°C	10s – 20s – 30s	39
Melting Curve	95° - 60° – 97°C	5s - 30s - contin.	1
Cooling	40°C	30 seconds	1

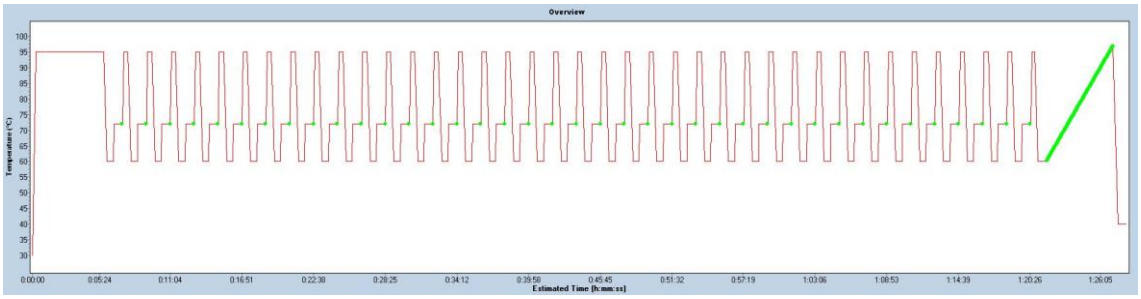

Figure 5: Illustration of the amplification-cycles run in qRT-PCR with temperature in °C and time

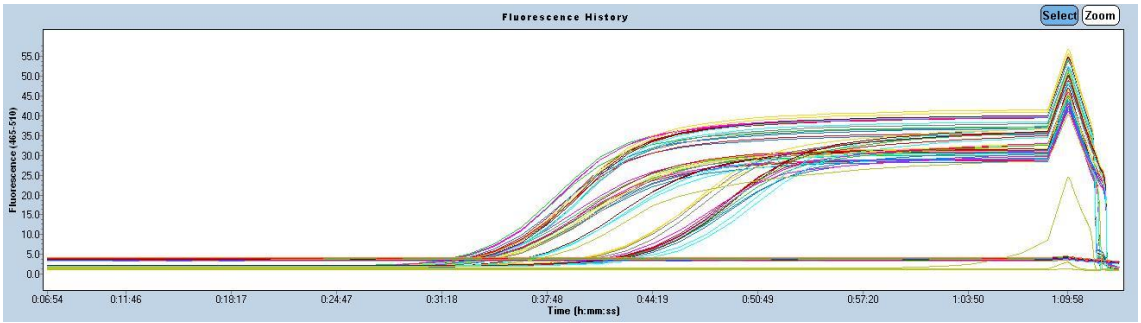

Figure 6: Melting curves of the samples displayed with fluorescence and time (s.c. amplification cycles)

Using the C_t-Value (cycle-threshold) and the level of expression of the reference genes, the relative expression of CD276 can be obtained as follows:

$$\Delta C_t = \Delta C_{t(CD276)} - \Delta C_{t(Reference-Gene)}$$

$$relative\ expression = 2^{(-\Delta C_t)}$$

2.8 Quantification of CD276 Protein

2.8.1 Protein Extraction

To analyze the protein CD276 in the observed cell lines quantitatively, a sodium dodecylsulfate polyacrylamide gel electrophoresis (SDS-PAGE) with a consecutive Western Blot was performed. Each cell line was cultured and processed to obtain a cell pellet as described in chapter 2.5. The pellet was then washed with 10 ml of approximately 4°C cold PBS and subsequently centrifuged at 200 g for 7 minutes. The pellet remained, which was suspended in 60-200 µl RIPA+ buffer depending on the size of the pellet. It was then stored for at least 24 hours at -80°C. Upon thawing, the samples were put on ice, transferred to a previously cooled centrifugation tube, and then centrifuged for 20 minutes at 4°C. The supernatant was transferred to another previously cooled centrifugation cup.

2.8.2 Protein concentration

To obtain the protein concentration in the samples, a Bradford Protein Assay was performed. A standard curve was obtained with standard concentrations according to Table 11.

Table 11: Standard concentrations for Bradford Protein Assay

Standard	Protein conc.
S1	3,04 mg/ml
S2	1,52 mg/ml
S3	0,76 mg/ml
S4	0,38 mg/ml
S5	0,19 mg/ml

The samples were diluted 1:4 or 1:5 with RIPA+ buffer. The results obtained were corrected for this dilution, respectively. In a 96-well microtitre plate per well 5 µl RIPA+ buffer for a blank, standard concentrations and samples were added. Next, 25 µl Reagent A' consisting of Reagent A with 2% Reagent S were added per well. Finally, 200 µl of Reagent B were added to each well, then the plate was placed on a mechanical shaker for 5 seconds and incubated for 15 minutes. Subsequently, the absorbance was measured at 650 nm with spectrophotometry and protein concentration values were obtained using the standard concentration curve. In new centrifugation tube, the samples were corrected to a protein concentration of 1 mg/ml with RIPA+ buffer. Laemmli buffer with 5% β-mercapthoethanol was added to a value of 32%. Finally, the samples were incubated for 10 minutes at 95°C and then stored at -20°C or immediately analyzed in a gel electrophoresis.

2.8.3 SDS-PAGE

The components for the 8% running SDS-gel were mixed according to Table 12 and incubated at room temperature for 30 minutes to enable polymerization. The 5% stacking SDS-gel components were mixed according to Table 13, transferred on top of the running gel and incubated for 30 minutes to enable polymerization.

Table 12: Components for 8% running SDS-gel for SDS-PAGE

Component	Percentage
Distilled water	45,9%
30% AcyramidMix	26%
1,5 M Tris, pH 8,8	26%
10% SDS	1%
10 % APS	1%
TEMED	0,1%

Table 13: Components for 5% stacking SDS-gel for SDS-PAGE

Component	Percentage
Distilled water	72%
30% AcyramidMix	16%
1,5 M Tris, pH 6,8	12%
10% SDS	0,1%
10 % Ammonium Persulfate	0,1%
TEMED	0,01%

After complete polymerization, the gels were put in a container with running buffer consisting of distilled water with 10% Tris-glycine and 0,1% 10% SDS solution. The gel was loaded with 25 µl of each sample from chapter 2.8.2. 5 µl Magic Mark was loaded as marker. The container was put on ice and the gel electrophoresis was run at 100 V for 90 min.

2.8.4 Western Blot

The stacking gel was removed and the running gel containing the separated proteins was transferred to a holding device together with a nitrocellulose membrane. The holding device was placed in a container filled with transfer buffer consisting of distilled water with 10% Tris-glycine and 20% methanol. The transfer was run at 100 V for 90 minutes. Immediately after the transfer, the membrane was washed 3 times for 10 minutes in phosphate buffered saline (PBS) solution and then placed in 5% milk powder solution for 1 hour in order to facilitate a specific antibody binding. The membrane was then washed in PBS containing 0,1% Tween20 3 times for 10 minutes and once in PBS for 10 minutes. A primary antibody targeting CD276 was diluted 1:600 in a 5% milk powder PBS solution, in which the membrane was incubated at 4°C on a shaking device overnight. Subsequently, the membrane was washed 3 times for 10 minutes in PBS containing 0,1% Tween20 and once for 10 minutes in PBS. A secondary rabbit anti-mouse horseradish peroxidase (HRP) antibody was

diluted 1:10000 in a 5% milk powder PBS solution, in which the membrane was placed for 1 hour at room temperature. Again, the membrane was washed 3 times for 10 minutes in PBS containing 0,1% Tween20 and once for 10 minutes in PBS.

To obtain a digital image of the membrane, Stable Peroxidase Solution and Luminol Enhancer Solution were mixed with equal volumes and pipetted on the membrane. After light protected incubation for 5 minutes, the membrane was placed on a C-DiGit® Blot scanner and an image was generated using the LI-COR® ImageStudio™ Lite software. To quantitatively analyze the Western Blot, signal intensities were measured for each individual band and the background was subtracted. After the image was acquired, the membrane was washed 3 times for 20 minutes in a specific stripping solution according to Table 4 and once for 10 minutes in PBS. For visualization of the β-actin bands as a reference and loading control, a primary antibody targeting β-actin was diluted 1:1000 in 5% milk powder PBS solution and incubated at 4°C overnight. The membrane was washed 3 times for 10 minutes in PBS containing 0,1% Tween20 and once for 10 minutes in PBS. A secondary goat anti-rabbit HRP antibody was diluted 1:2000 in 5% milk powder PBS solution, in which the membrane was incubated at room temperature for 1 hour. After the previously mentioned washing steps, a digital image of the membrane was acquired. Figure 11 shows the raw and analyzed image obtained.

Table 14: Antibodies, Manufacturer and Dilution for Western Blot

Antibody	Manufacturer/Reference Number	Dilution
Anti-CD276 antibody	abcam/ab105922	1:600
Anti-beta actin antibody	abcam/8227	1:1000
Rabbit anti-aouse Immunoglobulins/HRP	Dako/P0260	1:10000
Goat anti-rabbit Immunoglobulins/HRP	Dako/P0448	1:2000

2.9 Detection of Mycoplasma DNA with PCR

In order to exclude a possible contamination of cell cultures and samples, a PCR detecting deoxyribonucleic acid (DNA) from mycoplasma bacteria was performed. At 80% confluence, approximately 1 ml of growth medium was transferred to a centrifugation tube. After incubation at 94°C for 5 minutes, the tubes were centrifuged at 13000 g for 1 minute. The supernatant was transferred to a new tube. The PCR was prepared in a 96-well plate. 15 µL of a 23 µL master-mix (Table 15) were mixed with 8 µL SybrGreen and added to 2µL of template for a total of 25 µL per well.

Table 15: Composition of master-mix for MycoSpy qRT-PCR per well

Reagent	Volume
NTW	9,3 µl
Taq polymerase puffer	2,7 µl
primer mix	9 µl
internal control (700bp)	1 µl
Taq polymerase	1 µl

The PCR was run with features according to Table 16.

Table 16: Features of PCR run to detect mycoplasma DNA

Program	Temperature	Time	Cycles
Pre-Denaturation	94°C	60 seconds	1
Denaturation	94°C	30 seconds	35
Primer-Annealing	62°C	30 seconds	35
Polymerization	72°C	60 seconds	35
Final Elongation	72°C	3 minutes	1

A 2% agarose gel was prepared and 5 µL of Gel Red Nucleic Acid stain by Biotinum was added. A 100bp ladder was placed in one gel-pocket as reference. 10 µL of a PCR product from a sample was transferred to a gel-pocket together with 4 µL of loading buffer. The gel electrophoresis was run at 50 Volt for 30-60 minutes. The result was examined under UV-light. A band at 500bp would be proof of a mycoplasma contamination.

2.10 Quantification of the miRNA Transcription with qRT-PCR

2.10.1 miRNA Extraction

In order to quantify the level of miRNA transcription in selected cell lines, a qRT-PCR was performed. Cells were cultured, harvested and processed as described in chapter 2.5. The resulting pellet was washed in approximately 4°C cold PBS and subsequently centrifuged at 200 g for 5 minutes. The supernatant was removed and the pellet was suspended in 700 µl QIAzol lysis reagent. After incubation at room temperature for 5 minutes, 140 µl chloroform were added and mixed well. After incubation for 3 minutes at RT, a centrifugation step at 12000 g for 15 minutes at 4°C was performed. The upper aqueous phase was transferred to a new tube and 100% ethanol was added at 1,5 times the volume. The solution was transferred to a RNeasy mini spin column and centrifuged at 10000 g for 15 seconds. The flow-through was discarded and 700 µl RWT buffer were added. After centrifugation at 10000 g for 15 seconds the flow-through was discarded and 500 µl RPE buffer were added. The column was centrifuged at 10000g for 15 seconds and the flow-through was discarded. 500 µl RPE buffer were added and the column was centrifuged at 10000 g for 2 minutes. The column was transferred to a new tube and centrifuged dry at 10000 g for 1 minute. 40 µl RNAse-free water were added to the column and it was centrifuged at 10000g for 1 minute.

The probe was filled up to 100 µl with RNAse-free water and 350 µl RLT buffer were added and well mixed. 250 µl 100% ethanol were added and well mixed. The entire contents of the tube were transferred to a RNeasy mini elute spin column and it was centrifuged at 10000 g for 15 seconds. Flow-through and collection tube were discarded and the column was placed in a new collection tube. 500 µl RPE buffer were pipetted on the column, it was centrifuged at 10000 g for 15 seconds and the flow-through was discarded. 500 µl 80% ethanol solution was pipetted on the column and it was centrifuged at 10000 g for 2 minutes. Flow-through and tube were discarded and the column was placed in a new collection tube. The column was centrifuged with an open lid to dry the membrane at 13000 g for 5 minutes. Flow-through and tube were discarded. The column was placed in a 1,5 ml centrifugation tube, 14 µl RNAse-free water was pipetted on the center of the column and it was centrifuged at 10000 g for 1 minute. The samples were stored at -80°C for further processing.

2.10.2 Reverse Transcription of miRNA into cDNA

The miRNA concentration in the samples was measured using photospectometry. The concentration was corrected to 1 µg/µl miRNA with RNase-free water. 8µl of a master-mix (Table 17) was added to 2µl of each sample or negative control, respectively. In the PCR block, the reverse transcription step was performed at 42°C for 60 minutes, followed by the inactivation of the reaction at 95°C for 5 minutes. Subsequently, the samples were stored at -20°C until qRT-PCR performance.

Table 17: Composition of master-mix for transcription of miRNA to cDNA per sample

Reagent	Volume
5 x buffer	2 µl
H_2O	4,5 µl
enzyme mix	1 µl
spike-in control	0,5 µl

2.10.3 miRNA qRT-PCR

To obtain the efficiencies for the PCR-primers used for this qRT-PCR, a cDNA pool from all samples was created and a dilution series up to a dilution of 1:64 was set up. In a 96-well plate, for each well 3 µl of sample or negative control were mixed with 7 µl master-mix (Table 18). Each primer was tested twice. A positive control was performed. A standard curve was obtained and an efficiency was calculated using the LightCycler® 480 Software. Table 18 displays the primers and their efficiencies. Reference miRNAs were chosen according to Ratert et. al (2012).

Table 18: Primer efficiencies for miRNA qRT-PCR

Gene	Melting temperature (°C)	Primer efficiency
miR-29c-3p	60	1,775
miR-187-3p	60	1,66
miR-181b-5p	60	1,787
SNORD49a	60	1.9

The samples mentioned in chapter 2.10.2 were diluted 1:10. The target primers were miR-29c-3p and miR-187-3p. MiR-181b-5p and SNORD49a were used as reference primers, respectively. Results were normalized on both reference genes and on each reference gene individually. The sequences have not been released by the manufacturer. The qRT-PCR was run with features according to Table 20.

Table 19: Composition of master-mix for miRNA qRT-PCR per well

Reagent	Volume
2x SybrGreen	5 µl
Primer	1 µl
H_2O	1 µl

Table 20: Features of miRNA qRT-PCR with Temperature and Time

Program	Temperature	Time	Cycles
PCR initial heat activation	95°C	2 minutes	1
2-step-cycling denaturation	95°C	10 seconds	45
Extensions	56°C	60 seconds	45
Melting curve	40°C	60 seconds	1

2.11 CD276 Flow Cytometry

To determine the level of expression of CD276 on the cell surface, the mean fluorescent intensities of antibody marked cells were measured using flow cytometry. Selected cells were cultured, harvested and processed as described in chapter 2.5. However, instead of EDTA and TrypLE™ Select, Accutase with an incubation time of 9 minutes at 37°C and 5%CO_2 was used to loosen cells from the surface of the cell cultivation flasks. The pellet was suspended in PFEA buffer described in Table 4. For each cell line, 1,5 ml of the suspension containing around 40000-50000 cells was transferred to a centrifugation tube. A negative control was added. The tubes were centrifuged for 4 minutes at 300 g and the supernatant was decanted. 50 µl Gamunex was added. The tubes were incubated for 20 minutes at 4°C and protected from light. Subsequently, 1 ml PFEA buffer was added and mixed well. The tubes were centrifuged for 4 minutes at 300 g and the supernatant was decanted. The direct PE-labeled antibody targeting CD276 was diluted 1:20 with PFEA buffer and 50 µl of the solution was added to each tube. For the negative control, 50 µl of PFEA buffer were added. The contents were incubated light protected at 4°C for 20 minutes. 1 ml of PFEA was added. The tubes were centrifuged at 300 g for 4 minutes. The pellet was suspended in 300 µl of PFEA buffer. The mean phycoerythrin (PE) fluorescent intensities of the samples were subsequently analyzed using the LSR II Flow Cytometer System by BD Biosciences using FloJo™ v 7.1.

Table 21: Antibody, Manufacturer and Dilution for CD276 Flow-Cytometry

Antibody	Manufacturer/Reference Number	Dilution
PE anti-human CD276	BioLegend®/351004	1:20

2.12 Statistical Analysis

The software SPSS version 26.0 for Windows (SPSS Inc, IL, USA) was used for statistical analysis. Differences in the means were analyzed using Man-Whitney-Test or Student's *t* test with independent variables. Correlation analysis was performed using Spearman's rank-order correlation. Correlation was displayed as a value from -1 (linear negative correlation) to 1 (linear positive correlation) for ρ (*Rho*). All data with p values less than 0,05 were considered statistically significant.

3 Results

3.1 Duplication Rate and Cell Culture

Urothelial carcinoma cell lines *UC 5*, *UC 6*, *UC 9*, *UC 10*, *UC 13*, *UC 14*, *UC 15*, *UC 16* and somatic controls labelled "*HL*" for probes from ureter or "*BL*" for probes from urine bladder were successfully cultivated using appropriate medias and providing optimal conditions. Morphology of growth and rate of duplication per 24 hours was observed. No contaminations of cell cultures were observed.

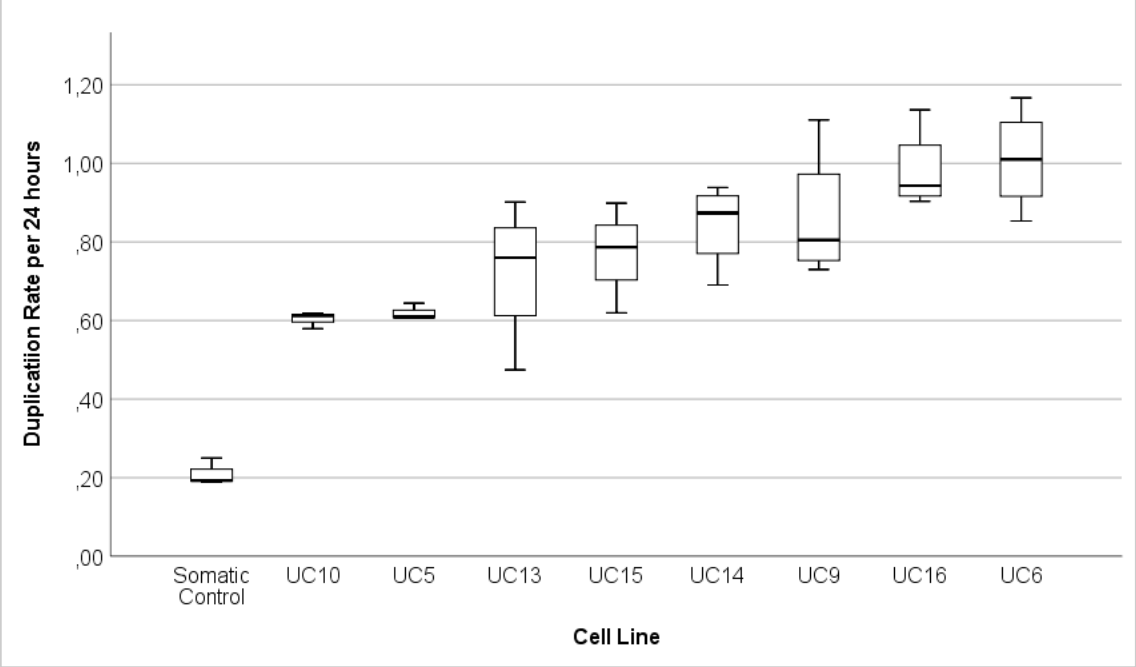

Figure 7: Median Duplication Rate per 24 hours in somatic (n=3) and UCC lines (n=29, n=3-5 per cell line).

Figure 7 displays the duplication rate of the examined cell lines. Somatic urothelial cells were duplicating at a median rate of 0,193/24h. All UCC lines had a higher duplication rate than somatic urothelial cells. *UC 6* and *UC 16* were duplicating fastest with a median DR of 1,01/24h and 0,943/24h, respectively. *UC 10* and *UC 5* were the slowest duplicating cancer cell lines with DRs of 0,612/24h and 0,608/24h, respectively. Correlation with other selected data is described in chapter 3.5.

Observation of morphology and pattern of growth revealed considerable differences. Somatic urothelial cell (**A**) exhibited a solitary and confined growth pattern and cells were only forming colonies in a later stage of cultivation. *UC 13* (**F**) displayed a similar growth pattern with a more fusiform appearance of cells (Figure 8).

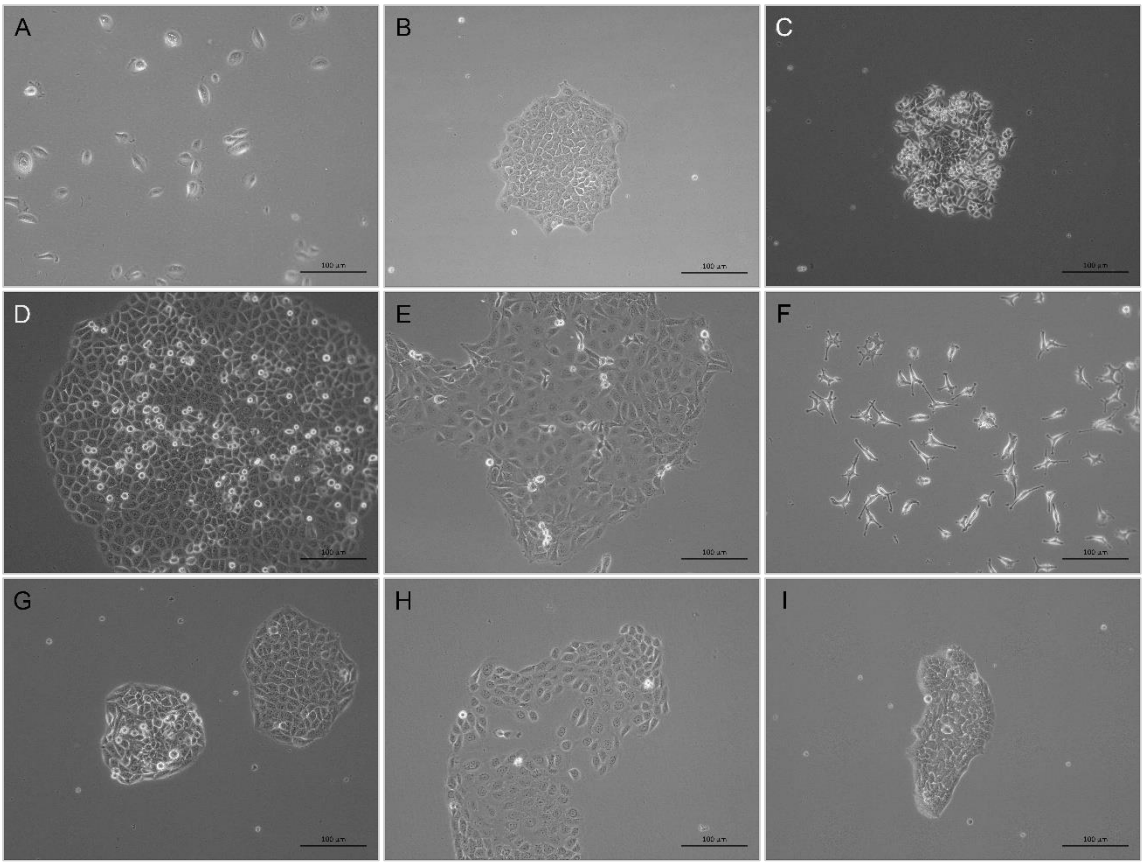

Figure 8: Cell cultures at day 7 post-seeding. ***A****: Somatic urothelial cells;* ***B****:UC 5,* ***C****:UC 6,* ***D****:UC 9,* ***E****:UC 10,* ***F****:UC 13,* ***G****:UC 14,* ***H****:UC 15,* ***I****:UC 16.*

While some cell lines evenly spread out, forming a homogenous monolayer, other cell lines grew in groups. Cell lines *UC 6* (**C**), *UC 10* (**E**) and *UC 15* (**H**) formed a loosely attached cluster of cells with some solitary cells. Cell lines *UC 5* (**B**), *UC 9* (**D**), *UC 14* (**G**) and *UC 16* (**I**) were forming tightly packed clusters of cells, even early in the cultivation phase. These cell lines also required a higher concentration of Trypsin with a longer incubation time in order to loosen cell-to-flask adherence. Almost no solitary, disseminated cells were detected.

As described in chapter 2.9, all cell cultures were tested for a possible contamination with *Mycoplasma* bacteria. All cell cultures used in this work were tested negative.

3.2 Expression of CD276 mRNA

To quantify the amount of CD276 mRNA expressed by each cell line, a qRT-PCR was performed. *PPIA* and *GAPDH* were chosen as stable reference genes. Somatic urothelial cells had a median CD276 mRNA expression of 0,1005 (0,707 – 0,1008).

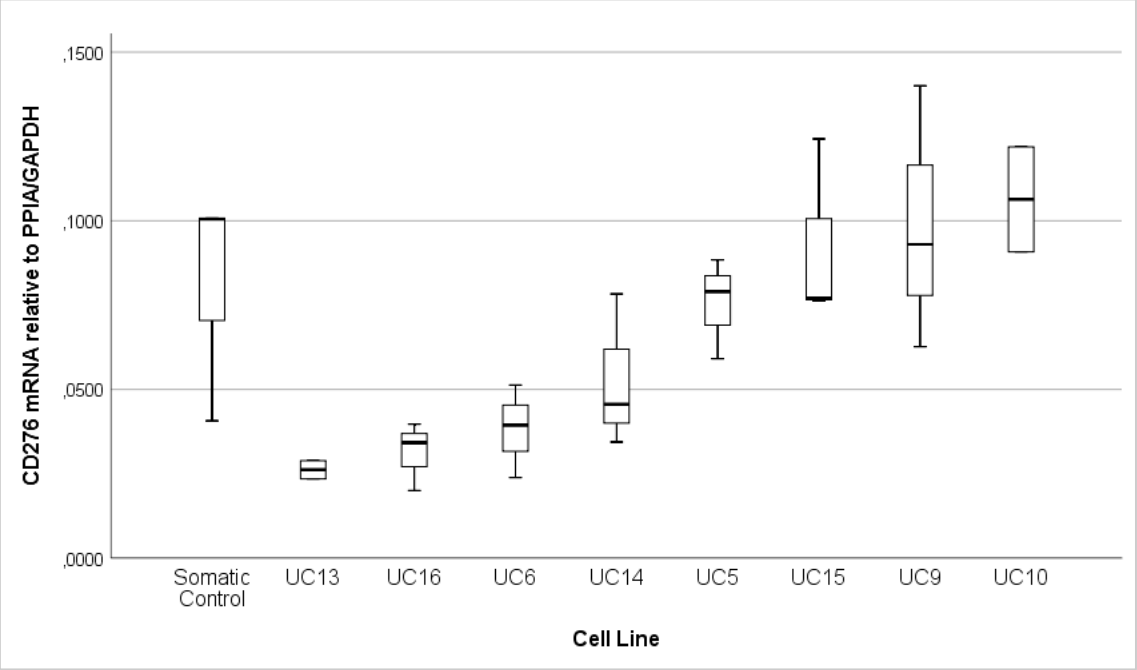

Figure 9:Median level of CD276 mRNA expression in somatic (n=4) and UCC cell lines (n=3 per cell line, except UC10 and UC13 n=2). Values are relative to reference genes PPIA/GAPDH.

As seen in Figure 9, only cell line *UC 10* had a higher level of median CD276 mRNA expression than somatic urothelial cells. A group of UCC lines consisting of *UC 9*, *UC 15* and *UC 5* expressed a moderate level of CD276 mRNA. UCC lines *UC 14*, *UC 6*, *UC 16* and *UC 13* had a median CD276 mRNA expression of 50% or lower than somatic urothelial cells. Exact values of all analyzed cell lines are displayed in Table 22. Overall median expression in UCCs was 0,061 (0,034 – 0,089) and therefore lower than median expression in somatic urothelial cells (0,101 (0,707 – 0,101), as displayed in Figure 10. Correlation with other selected data is described in chapter 3.5.

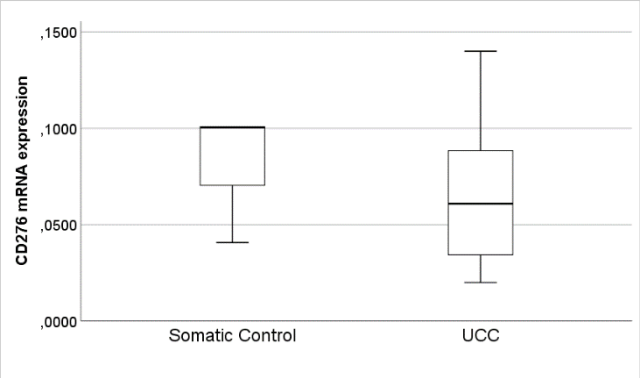

Figure 10: Median level of CD276 mRNA expression in somatic urothelial cells (n=4, 0,101 (0,707 – 0,101)) and UCCs (n=22, 0,061 (0,034 – 0,089)). Values are relative to reference genes PPIA/GAPDH.

Table 22: Median CD276 mRNA expression of analyzed UCC lines and somatic control cells with percentiles.

Cell Line	Median CD276 mRNA expression
Somatic Control	0,1005 (0,707 – 0,1008)
UC 13	0,026 (0,023 – 0,029)
UC 16	0,034 (0,027 – 0,037)
UC 6	0,039 (0,031 – 0,045)
UC 14	0,045 (0,040 – 0,061)
UC 15	0,077 (0,076 – 0,100)
UC 5	0,079 (0,069 – 0,084)
UC 9	0,093 (0,077 – 0,116)
UC 10	0,106 (0,090 – 0,121)

3.3 Expression of CD276 Protein

To quantitively asses the amount of CD276 Protein expression in each cell line, an SDS gel electrophoresis followed by a Western Blot immunoblot was performed. Somatic urothelial cells from clinically tumor free bladder and ureter tissue served as control.

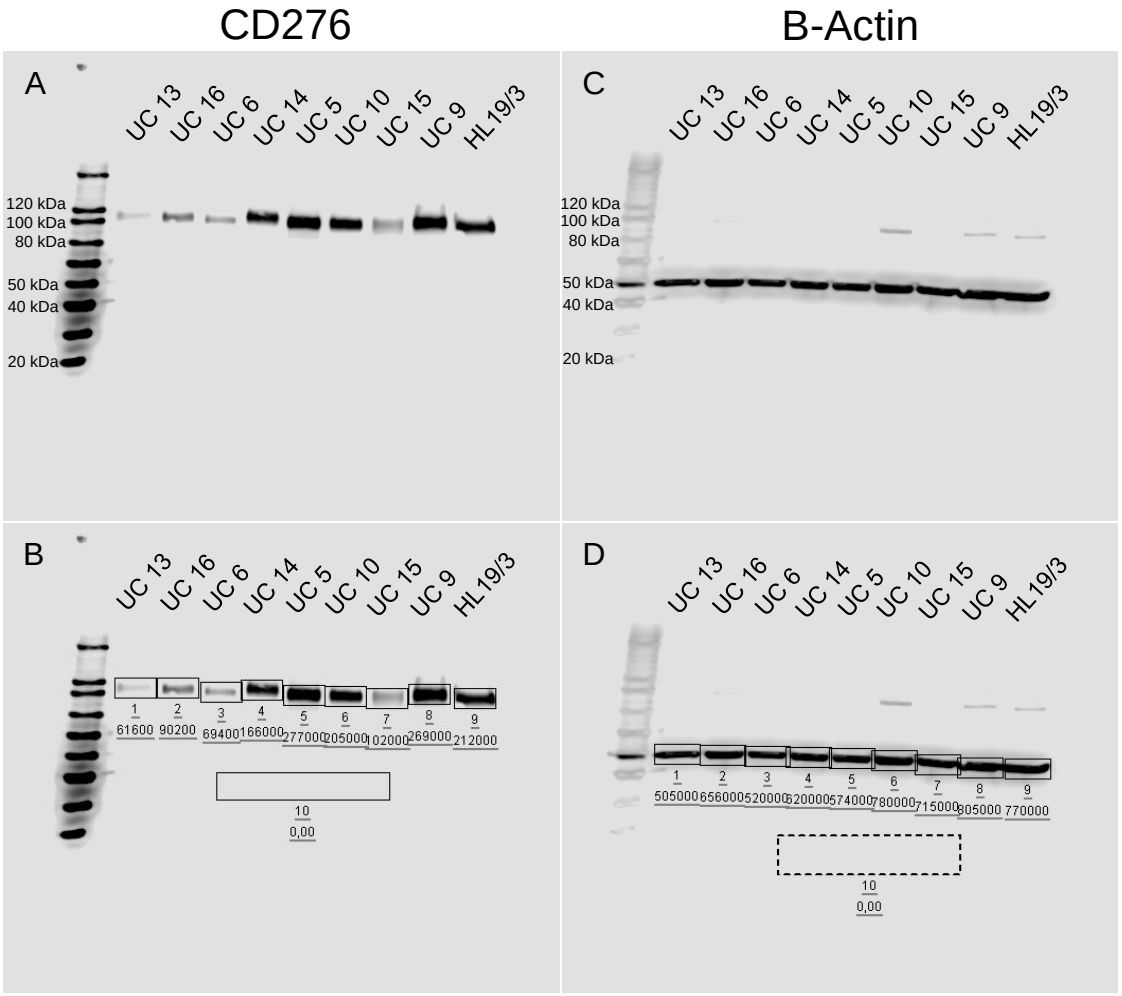

*Figure 11: Western Blot for CD276 and b-actin. **A**: Immunoblot with antibodies staining CD276 and bands at 120 kDa. **B**: Evaluation of CD276 staining intensity with Image Studio™ Lite software. **C**: Immunoblot with antibodies staining b-actin and bands at 50 kDa. **D**: Evaluation of b-actin staining intensity with Image Studio™ Lite software.*

CD276 protein expression was calculated as a ratio of CD276 to b-actin, as b-actin was proven to be a stable housekeeping gene with a steady level of expression in different types of cells.

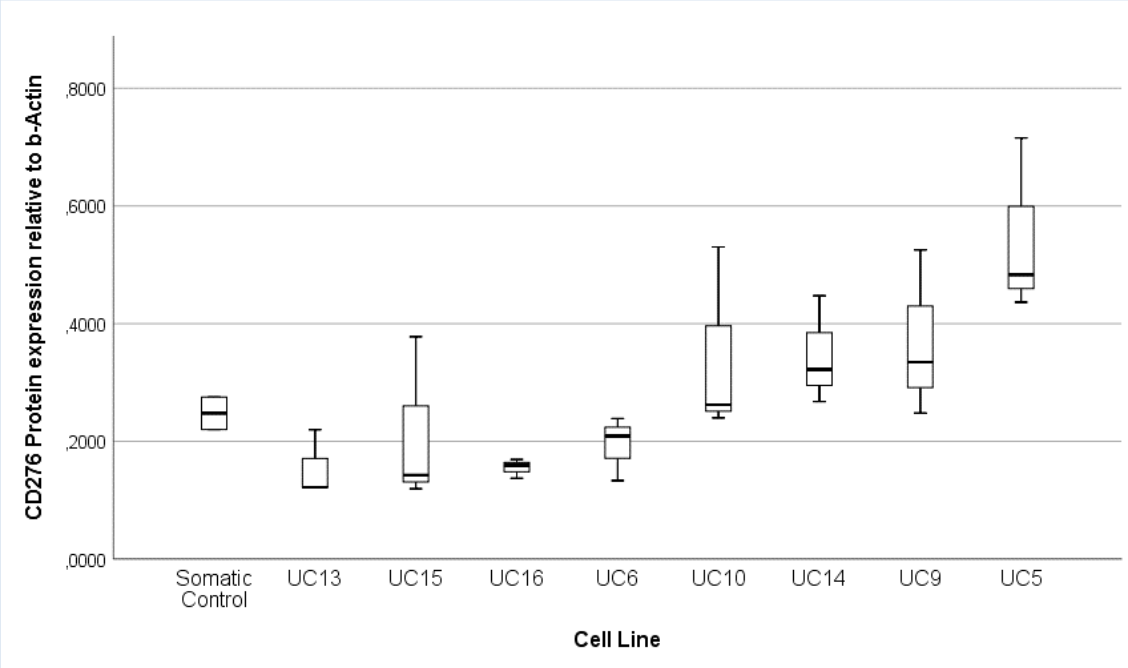

Figure 12: Median CD276 protein expression in UCC lines (n=3 per cell line) compared to somatic urothelial cells (n=2). Level of expression is displayed as ratio to b-Actin protein expression.

UCC lines can be sorted into groups according to their level of protein expression. *UC 5* had the highest level of protein expression relative to β-actin with around twice as much as somatic urothelial cells. A group consisting of *UC 9*, *UC 14* and *UC 10* expressed CD276 protein slightly higher than somatic urothelial cells. The last group of cells consists of *UC 6*, *UC 16*, *UC 15* and *UC 13* with protein expression lower than somatic urothelial cells. Figure 12 shows the median CD276 protein expression according to cell line. Figure 13 displays the median protein expression of all analyzed UCCs compared to somatic urothelial cells. Correlations with other analyed data are described in 3.5.

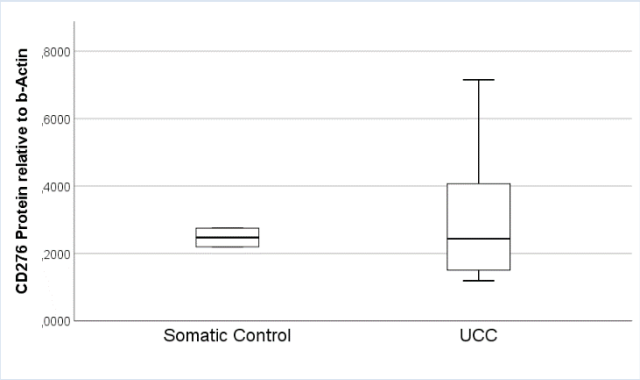

Figure 13: Median level of CD276 protein expression in somatic urothelial cells (n=2, 0,247 (0,220 – 0,275)) and UCCs (n=24, 0,244 (0,155 – 0,392)). Values are relative to reference gene b-Actin.

Table 23: Median CD276 protein expression relative to b-Actin by cell line.

Cell Line	Median CD276 Protein relative to b-Actin
HL 19/3 (Somatic Control)	0,247 (0,220 – 0,275)
UC 13	0,12204 (0,12201 – 0,170)
UC 15	0,142 (0,131 – 0,260)
UC 16	0,159 (0,148 – 0,168)
UC 6	0,209 (0,171 – 0,224)
UC 10	0,262 (0,251 – 0,396)
UC 14	0,322 (0,295 – 0,384)
UC 9	0,334 (0,291 – 0,430)
UC 5	0,483 (0,460 – 0,600)

3.4 Expression of CD276 on the Cell Surface

The molecule CD276 is ultimately transported to the cell surface and integrated in the cell membrane. To quantify the expression of CD276 on the cell surface, staining with fluorescent antibodies and subsequent measurement of mean fluorescence using Flow-Cytometry was carried out.

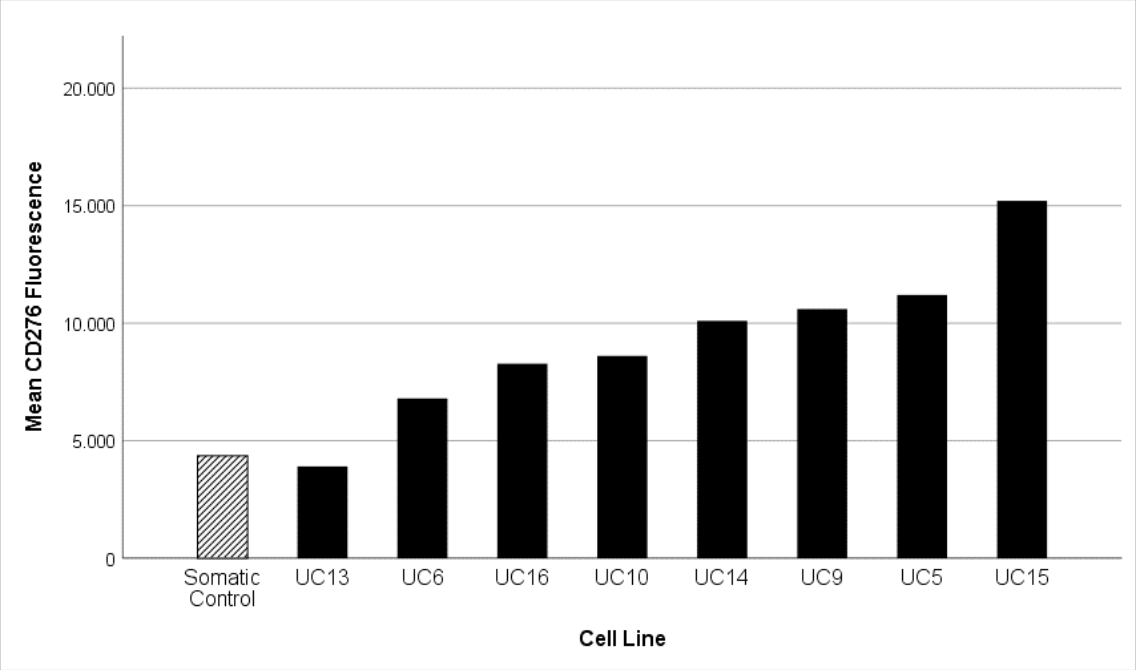

Figure 14: Mean CD276 fluorescence intensities on cell surface of somatic urothelial cells (n=1) and UCCs (n=1 per cell line) by cell line.

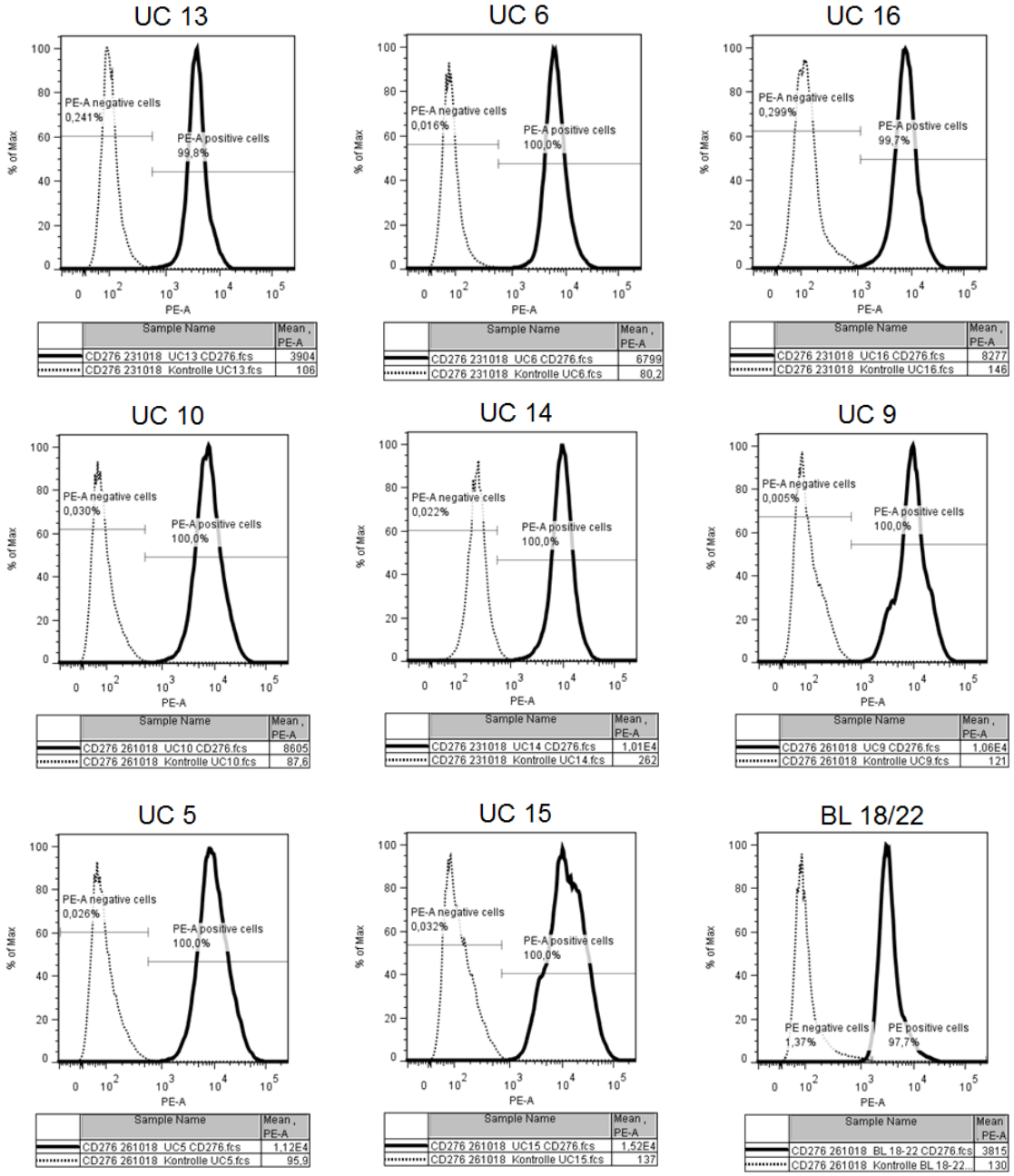

Figure 15: Mean fluorescence intensities of UCC lines stained with anti-CD276 antibodies. BL 18/22 is displayed as exemplary urothelial control cell. Left peak shows the negative control, right peak shows the PE-A positive cells.

Figure 15 shows the mean fluorescence of somatic urothelial cells and UCC lines stained with anti-CD276 antibodies and analyzed by flow cytometry. Controls with IgG1 isotype staining provided evidence for specific binding of this antibody (not shown). *UC 13* was the only cell line with a mean fluorescence intensity less than that of somatic urothelial cells. *UC 6*, *UC 16* and *UC 10* all had a moderate fluorescent intensity of around 8000, which is around twice as

much as somatic urothelial cells. *UC 14*, *UC 9* and *UC 5* had a high expression on the surface with a mean fluorescence intensity of around 10000. The highest mean fluorescent intensity was emitted by cell line *UC 15* with around 15000. Exact values are displayed in Figure 14 and Table 24. The overall median fluorescence intensity of all UCCs stained with anti-CD276 antibodies was 9352,5 (7538 – 10900), therefore around twice as much as that of somatic urothelial cells (see Figure 16). Correlation with other data is displayed in chapter 3.5.

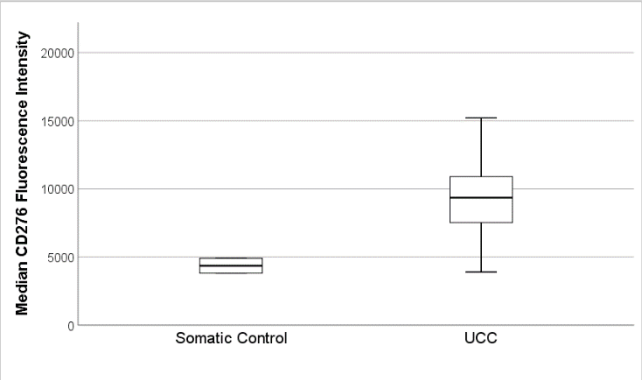

Figure 16: Median CD276 fluorescence intensity of somatic urothelial cells (n=2, 4361 (4088 – 4634)) and UCCs (n=8, 9352,5 (7538 – 10900)).

Table 24: Mean CD276 fluorescence intensities of analyzed cells.

Cell Line	Mean CD276 fluorescence intensity
Somatic Control (HL 18/24 + BL 18/22)	4361
UC 13	3904
UC 6	6799
UC 16	8277
UC 10	8605
UC 14	10100
UC 9	10600
UC 5	11200
UC 15	15200

3.5 Correlation of CD276 mRNA-, Protein- and Surface-Expression

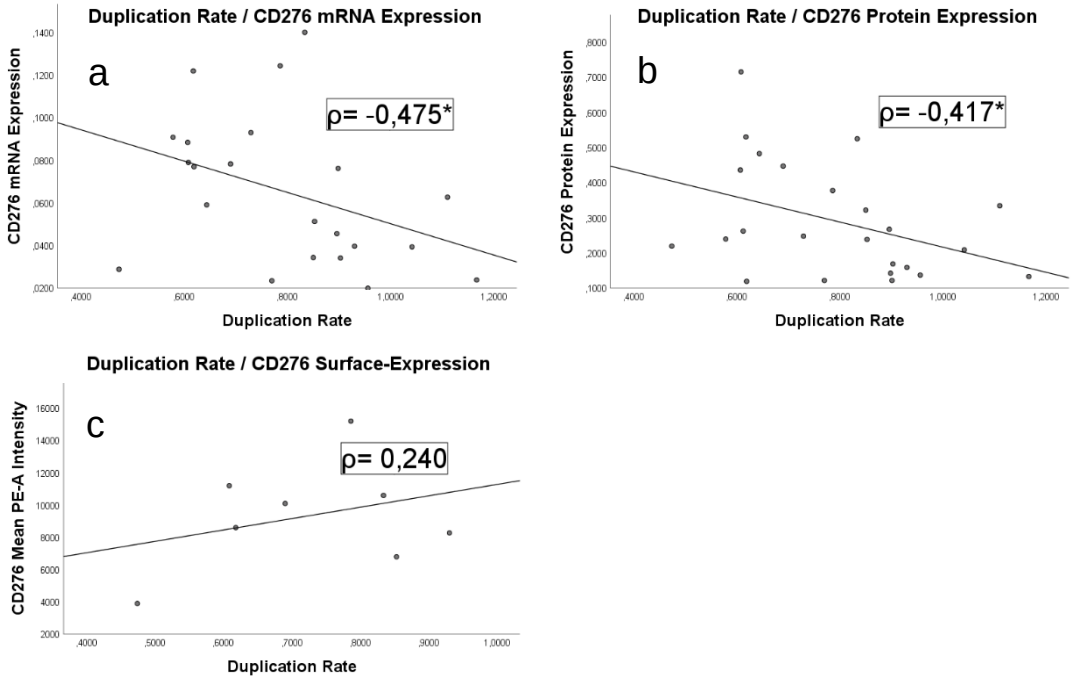

*Figure 17: Correlation of duplication rate with selected data. Each point represents data for a specific cell line and measurement. ρ=Spearman's rank correlation coefficient. Addition of linear trend line. *Correlation is significant at the 0,05 level.*

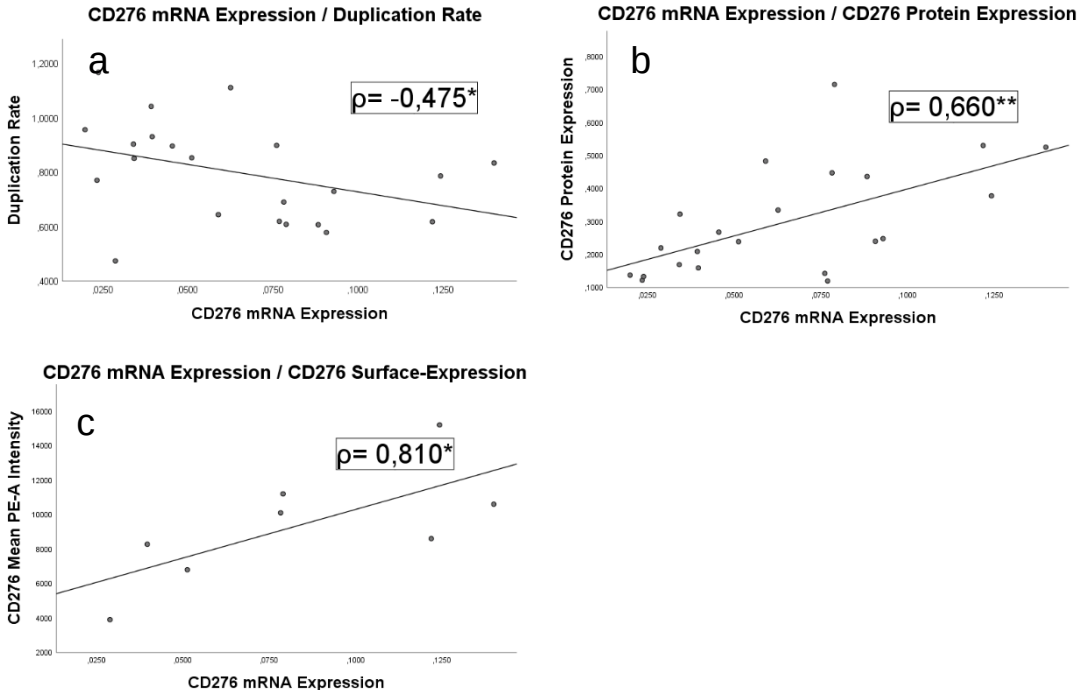

Figure 18: Correlation of CD276 mRNA expression with selected data. ρ=Spearman's rank correlation coefficient. Each point represents data for a specific cell line and measurement. ρ=Spearman's rank correlation coefficient. Addition of linear trend line.
** Correlation is significant at the 0,05 level ** Correlation is significant at the 0,01 level*

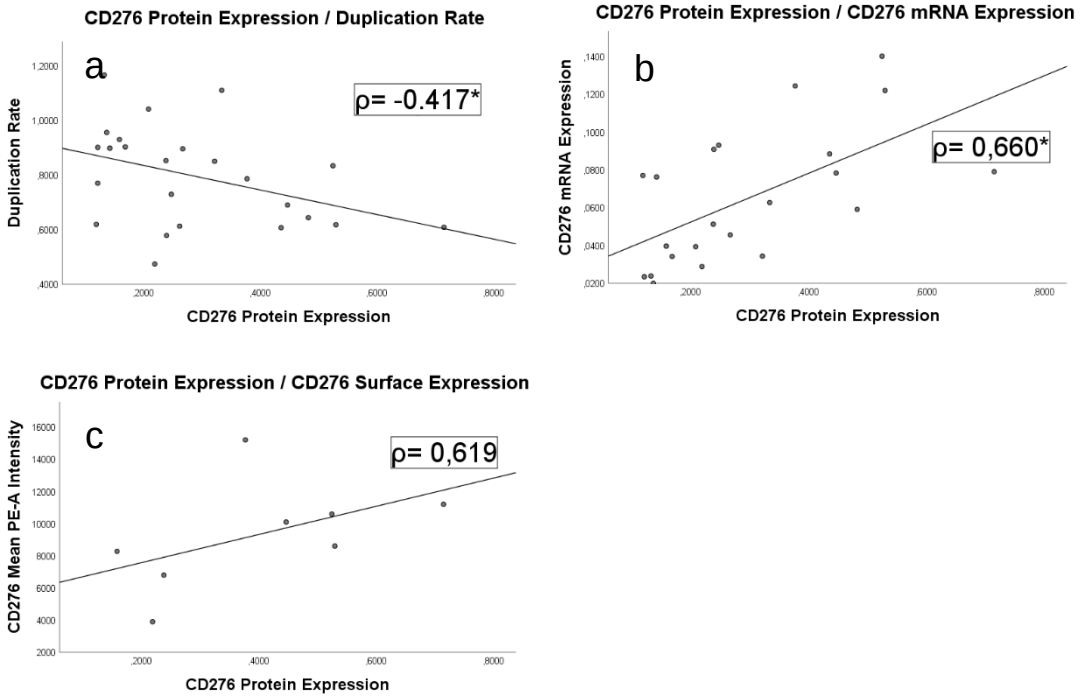

*Figure 19: Correlation of CD276 protein expression with selected data. ρ=Spearman's rank correlation coefficient. Each point represents data for a specific cell line and measurement. ρ=Spearman's rank correlation coefficient. Addition of linear trend line. * Correlation is significant at the 0,05 level*

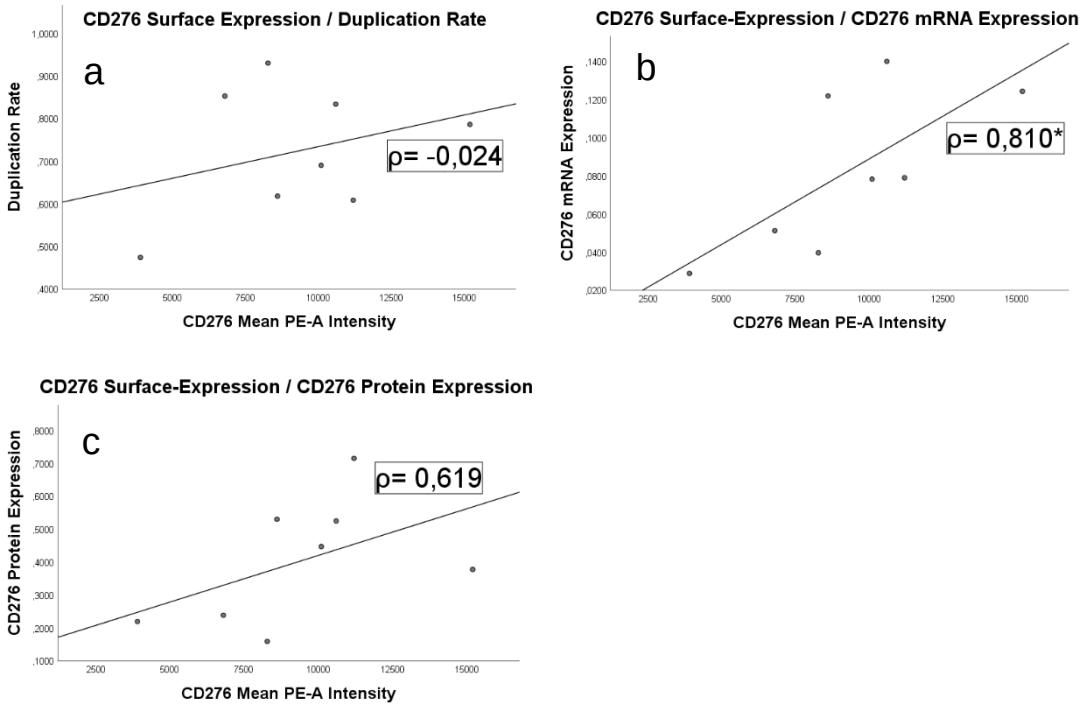

*Figure 20: Correlation of CD276 surface-expression with selected data. ρ=Spearman's rank correlation coefficient. Each point represents data for a specific cell line and measurement. ρ=Spearman's rank correlation coefficient. Addition of linear trend line. * Correlation is significant at the 0,05 level*

In order to evaluate if the data obtained were in correlation with each other, a Spearman's correlation coefficient was obtained. Figure 17, Figure 18, Figure 19 and Figure 20 graphically illustrate the correlation and the correlation coefficient. Data obtained from a certain cell line in a category (e.g. duplication rate) is displayed with data of another category (e.g. CD276mRNA expression) obtained from the same cell line as a single dot in the graph. A linear trend line has been added to visualize the correlating trend. The correlation itself is best represented by Spearman's correlation rank coefficient (*ρ)*. Duplication rate of cells had a significant negative correlation with CD276 mRNA expression (*ρ*=-0,475) and CD276 protein expression (*ρ*=-0,417). It correlated positively with CD276 surface-expression (*ρ*=0,240), however not statistically significant.

CD276 mRNA expression correlated moderately positive with CD276 protein expression (*ρ*=0,660) and strongly positive with CD276 surface-expression (*ρ*=0,810). Furthermore, CD276 protein expression correlated moderately positive with CD276 surface-expression (*ρ*=0,619), however not statistically significant.

3.6 miRNA Primer Efficiencies and Reference miRNAs

To the best of my knowledge, most of the in 2.10 mentioned miRNA primers have not been tested on the UCC lines investigated in this thesis. In a first step, it was to be evaluated, whether these primers were working in a PCR with the genetic material obtained by the UCCs. A primer efficiency at a melting temperature of 60°C had to be obtained.

Out of all primers tested on a cDNA pool of UCC lines *UC 6, UC 16, 5637, Cal-29, TCC, 253J* and *HT1197*, only primers for *miRNA 29c*, *miRNA 187*, *miRNA 181b* and *SNORD49a* were able to produce results. Calculated primer efficiencies are shown in Table 18. An exemplary standard curve is displayed in Figure 21.

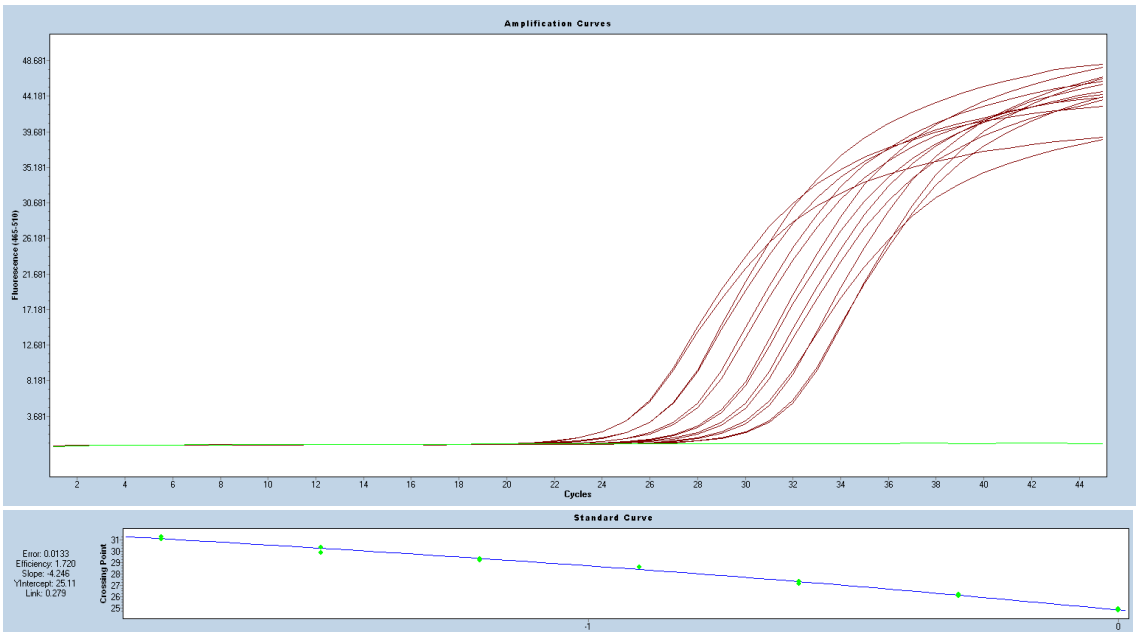

Figure 21: Exemplary qRT-PCR amplification curve with a calculated standard curve for miR-181b-5p.

3.7 Expression of miRNA 29c and miRNA 187

To quantify the expression of miRNA 29c and miRNA 187 in UCC lines and somatic urothelial cells, a qRT-PCR was run. *MiR 181b* and *SNORD49a* were used as reference genes. Values were normalized on somatic urothelial cell expression to visualize divergences.

3.7.1 Expression of miRNA 29c

Figure 23 shows the expression of *miRNA 29c* in selected UCC lines compared to urothelial cells. All cell lines, except *253J*, show an expression lower than that of urothelium. *Cal-29* and *HT1197* are cell lines expressing miRNA 29c the lowest. *UC 6*, *UC 16* and *5637* have a moderate expression of miRNA 29c. *TCC* expression is slightly lower, and *253J* moderately higher than that of urothelium. Table 25 shows the exact mean values with standard deviation. Median expression of *miRNA 29c* in UCC lines combined was significantly lower compared to expression in somatic urothelium (see Figure 22).

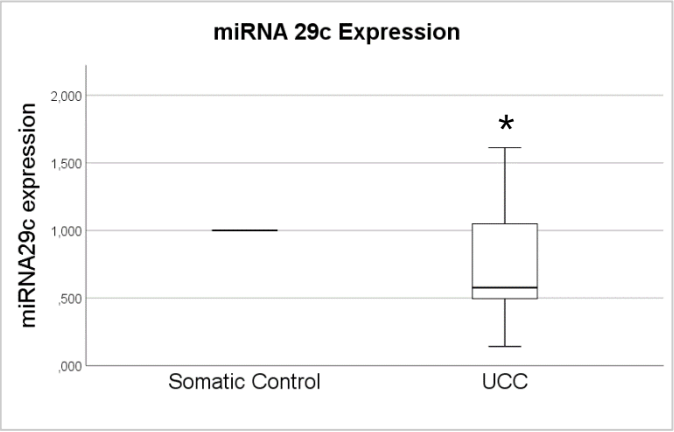

*Figure 22: Relative median expression of miRNA 29c in UCC cell lines (n= 20, 0,577 (0,484 – 1,193)) compared to somatic urothelium (n=4, 1,00). Normalized on somatic urothelium. *p<0,05*

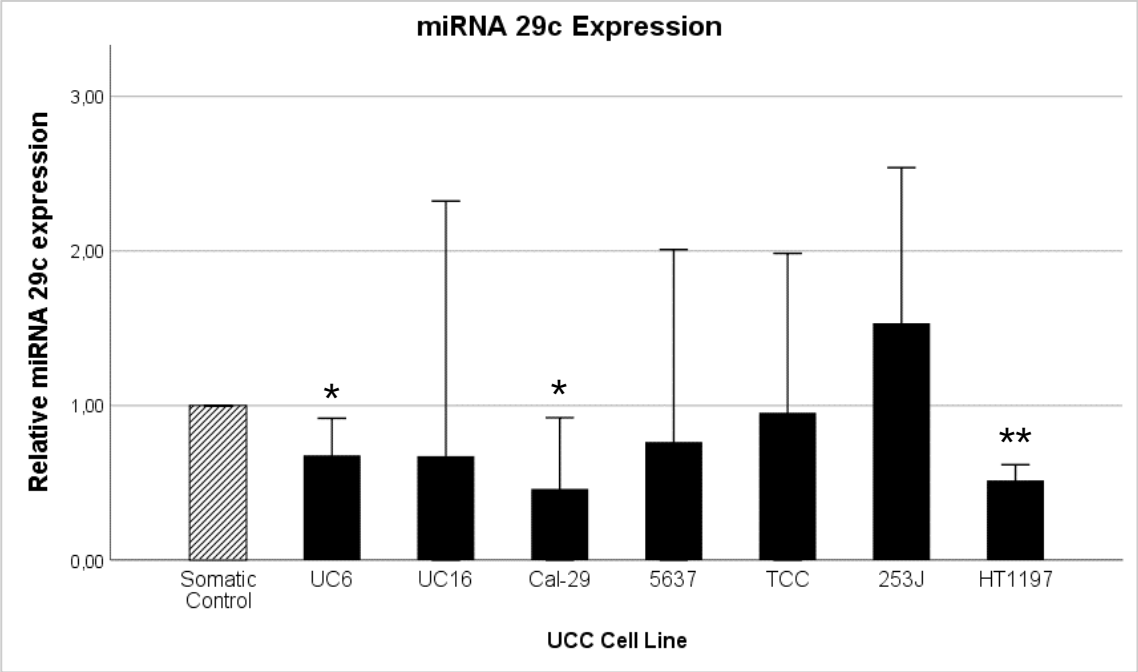

*Figure 23: Relative mean expression of miRNA 29c in UCC cell lines (n=3 per cell line, except 253J n=2) with standard deviation. Values are normalized on somatic urothelial control cells. *p<0,05, **p<0,01*

3.7.2 Expression of miRNA 187

Figure 24 shows the expression of *miRNA 187* in UC compared to somatic urothelium, respectively. UCC line *TCC* shows no detectable expression of *miRNA 187*, cell line *253J* shows minimal expression of *miRNA 187*. *UC 16* and *5637* express *miRNA 187* at a low level compared to somatic urothelium. *UC 6*, *Cal-29* and *HT1197* have higher expression levels than somatic urothelial cells with *HT1197* having the highest expression out of all examined cell lines. Standard deviation for cell lines *Cal-29* and *HT1197* show high values. Median expression of *miRNA 187* in all examined UCC lines

*Figure 24: Relative median expression of miRNA 187 in UCC cell lines (*n*=15, 0,156 (0,005 – 1,415)) compared to somatic urothelium (*n*=4, 1,00). Normalized on somatic urothelium.*

was lower compared to expression in somatic urothelial cells, however not significantly. Table 25 displays the exact mean expression values with standard deviation.

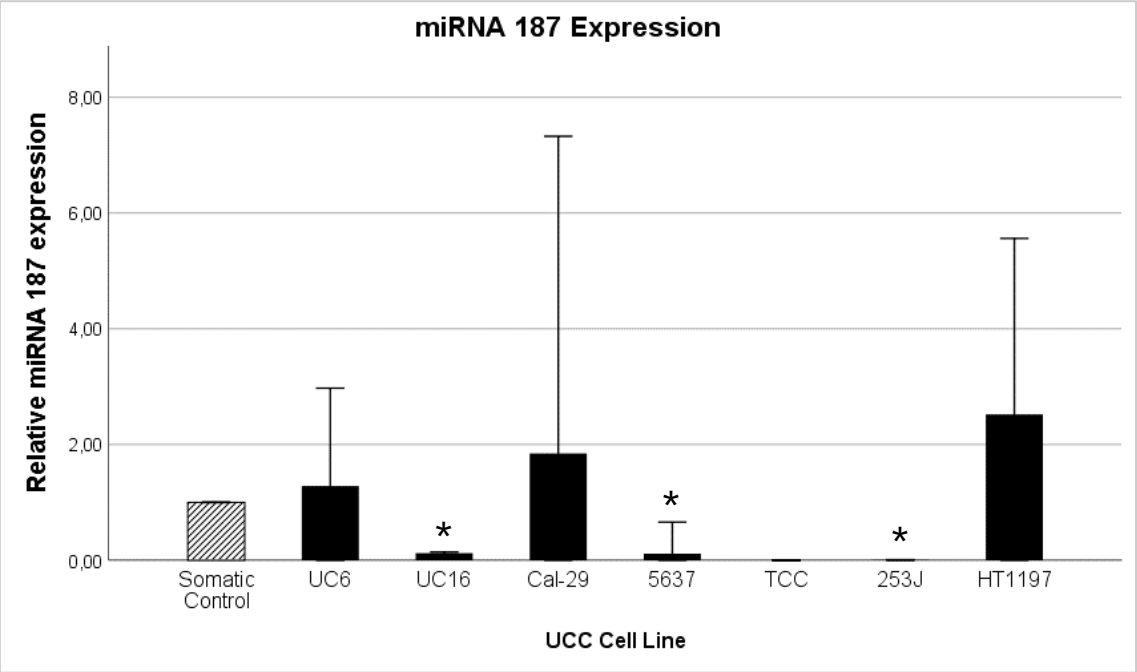

*Figure 25: Relative mean expression of miRNA 29c in UCC lines (n=2 per cell line, HT1197 n=3) and somatic urothelium (n=4) with standard deviation. Values are normalized on somatic urothelial control cells. *p<0,05*

Table 25: Mean miRNA 29c and miRNA 187 expression of UCC lines and somatic urothelial cells (HL). Results are normalized on somatic urothelium and standard deviation is displayed. (HL=Harnleiter)

Cell Line	miRNA 29c	miRNA 187
Somatic Control (HL 19/3 + HL 19/15)	1,000 (0,000)	1,000 (0,000)
UC 6	0,677 (0,096)	1,281 (0,133)
UC 16	0,672 (0,664)	0,123 (0,002)
Cal-29	0,460 (0,185)	1,845 (0,609)
5637	0,764 (0,501)	0,113 (0,060)
TCC	0,953 (0,415)	0,000 (0,000)
253J	1,533 (0,111)	0,005 (0,001)
HT1197	0,515 (0,041)	2,521 (1,223)

4 Discussion

4.1 UCC Line Selection and Morphology

The reasons for choosing specific established cell lines were diverse. First of all, the goal was to provide a base for further research focusing on CD276. Established cell lines can give studies a higher inter-experimental comparability. Growing conditions of these cell lines can be standardized. Also, these cell lines are readily accessible. Ethical concerns and errors in methods (e.g. sample collection) can be decreased (Kaur and Dufour, 2012). Previous work on CD276 was carried out on other selected UCC lines. To the best of my knowledge, the data obtained in this work has not been obtained on these specific UCC lines up to this date. However, the downside of working with established cell lines is, that results obtained cannot be directly linked to a patient's history or other clinical data. Even today, a lot of cell lines are subject to cross-contamination and presents a problem when working with established cell lines (Capes-Davis et al., 2010).

As described in chapter 3.1, the morphology of the cells in culture was different for each cell line. Cell line *UC 13* was the only cell line, which did not organize into groups or clusters (Figure 8). Remarkably, it was also the cell line expressing CD276 lowest on mRNA, protein and cell surface level out of all cell lines examined. CD276 could potentially also play a role in the structure and organization of tumor cells. Cell lines *UC 6*, *UC 10* and *UC 15* were forming loosely attached colonies. It may be possible, that in these cell lines the epithelial-mesenchymal-transition (EMT) is further progressed than in the cell lines forming tightly packed colonies. Observations supporting this hypothesis were made during cell processing. Cell line *UC 5* was forming a tightly packed

cluster of cells and when treated with proteases in order to loosen cell-to-cell and cell-to-ground connections, this cell line had to be treated with a higher concentration and longer incubation time than other cell lines.

Elevated CD276 is known to correlate with low E-cadherin expression in tumor cells (Jiang et al., 2016b). Another hypothesis is that these cell lines might be taken from a tumor at a higher stage, in which migration was further progressed than in tumor cells at a lower stage. However, no clinical correlation can be made in this case. As expected of tumor cells, all UCC lines had a higher proliferation rate than somatic urothelial cells *in vitro*. However, proliferation of cells correlated moderately negative with CD276 expression on mRNA and protein level. This may seem controversial, as in the literature, CD276 expression correlated with proliferation marker *Ki-67* in epithelial tumor cells (Pizon et al., 2018) and is associated with increased tumor proliferation and progression (Dong et al., 2018). CD276 does not seem to control the proliferation of bladder cancer cells. Another explanation for this discrepancy may be the difference in the microenvironment between *in vitro* and *in vivo* growth. The molecular mechanisms, by which CD276 facilitates tumor growth and progression are beneficial for tumors *in vivo*. Mechanisms for degradation of the ECM are powerful tools of tumor cells for the process of migration and invasion. However, overexpression of MMPs (Tekle et al., 2012) or increasing *IL-8* and *VEGF* expression (Xie et al., 2016) will most likely not help cells proliferate in cell culture flasks. Moreover, slower and potentially more organized growth may help tumor cells in evading the immune system or keeping selection pressure low. In cell culture, somatic urothelial cells are maintained in media facilitating proliferation. Thus, at least *in vitro*, normal cells are possibly dividing at unphysiologically high rates. This may distort analyses of correlations between expression of CD276 and cell proliferation of both, somatic urothelial cells as well as UCC lines. This hypothesis is corroborated by our recent preliminary studies showing high CD276 expression in the slow growing UCC line HT1197 (unpublished observation from different research group in the laboratory of Prof. Dr. Aicher, not shown).

4.2 CD276 Expression

Results of the qRT-PCR for CD276 mRNA showed a variable expression in the selected UCC lines. All UCC lines, except *UC 10,* expressed a median CD276 mRNA level equal or less than somatic urothelial cells. Unfortunately, no connection to tumor stage can be made in these selected UCC lines, as for most cell lines tumor stage is unkown. As CD276 mRNA expression is associated with tumor stage in bladder cancer (Li et al., 2017), it is likely that the UCC lines investigated are taken from a tumor at a lower stage. CD276 mRNA expression as a biomarker for bladder cancer has therefore to be viewed critically. However, it could be a useful marker for differentiation of tumor cells into higher or lower tumor stages in bladder cancer samples.

The origin of somatic urothelial cells was confirmed via AE1/AE3 staining and a possible tumor transformation is very unlikely. A possible population of sub-clones may have developed in the UCC cell lines, as they have undergone passaging multiple times (e.g. *UC 6* 109 times or more). As mentioned in chapter 3.1, contamination with *mycoplasma* bacteria and a consequent down- or up regulation of CD276 mRNA expression has been considered and ruled out by testing of cell cultures. This is especially important, since CD276 was observed to be elevated in children with *mycoplasma* pneumonia (Chen et al., 2013). In cutaneous melanoma, CD276 was found to be involved in epigenetic regulatory activity (Wang et al., 2013). A possible epigenetic regulation of CD276 expression itself must be considered, as well. Overall, the analyzed UCC lines could be useful, when examining possible mechanisms of upregulation of CD276. Changes in CD276 expression (e.g. upregulation) by altering molecular mechanism would be observed very prominently in these UCC lines.

Examination of CD276 protein expression of the selected UCC lines yielded no clear linear results expected from CD276 mRNA expression. SiRNA and miRNA most likely play a post-transcriptional role in the regulation of CD276 expression

and are further discussed in chapter 4.4. Cell line *UC 13* expressed CD276 on mRNA and protein level lowest out of all cell lines examined. In this cell line it can be assumed, that post-transcriptional regulation does not play a significant role. Equally, *UC 6* and *UC 16* have very low expression levels of CD276 mRNA and protein, suggesting only a minor post-transcriptional regulation. *UC 5*, *UC 9*, *UC 10*, *UC 14* and *UC 15* will have to be subjects to further studies concerning miRNA regulation. All in all, calculated correlation shows a moderate association of CD276 mRNA and protein expression, which supports the hypothesis of other regulatory factors, such as miRNAs.

In contrast to CD276 expression on mRNA and protein level, expression of CD276 on the surface of cells was remarkably higher for UCC cells. Only cell line *UC 13* had a lower expression on the surface when compared to somatic cells, forming a link to its equally low expression of CD276 on mRNA and protein levels. The noticeably higher findings for the remaining UCC lines indicate further mechanisms beyond regulation by miRNAs. There is a strong correlation between CD276 mRNA expression and CD276 surface expression (Spearman's $\rho=0{,}810$, $p<0{,}05$) and an only moderate and not significant correlation between CD276 protein expression and CD276 surface expression (Spearman's $\rho=0{,}619$, $p>0{,}05$). CD276 protein expression as a biomarker may therefore not be able to yield reliable information. CD276 mRNA expression combined with CD276 surface expression will most likely give the most accurate information about levels of CD276 in a tumor cell.

For another member from the superfamily of immune checkpoint molecules, PD-L1, multiple regulating factors have been identified. *IFN-γ*, *STAT-1* and *JAK* pathways were shown to regulate PD-L1 expression on a transcriptional and post-transcriptional level (Mamessier et al., 2018). However more importantly, two studies identified *CMTM6* (Chemokine-like factor-like (CKLF) MARVEL Transmembrane domain containing family Member 6) as a regulator of expression at the cell membrane without modifying mRNA expression levels (Burr et al., 2017, Mezzadra et al., 2017). *CMTM6* had a stabilizing effect on PD-L1 by preventing its ubiquitination. Similar regulators will have to be

explored for CD276 and the resulting data may be able to explain the variable expression levels. Other mechanisms of regulation or induction may be hypoxia or the exposure to lipopolysaccharides (LPS) from gram-negative bacteria. These bacteria are also the main pathogens associated with urinary tract infections. Until further regulation is explored, anti-CD276 therapy should aim at the surface of tumor cell to exhibit a maximum therapeutic effect. In normal urothelium from patients with UC >pT3a, CD276 expression is significantly lower than in UC <pT3a, recommending a use of anti-CD276 therapy in later stages (Aicher et al., 2021). Overall, UCC cell lines will have to be chosen carefully in future studies and variances between different cell lines will have to be considered.

4.3 Establishing miRNA Target and Reference Genes

To quantify miRNA expression levels in the selected UCC lines, primer efficiencies for a subsequent qRT-PCR had to be established. According to Ratert et. al (2012), several references miRNAs had been identified in urothelial cell carcinomas. These included a combination of four (*miR-101*, *miR-125a-5p*, *miR148b*, and *miR-151-5p*) or three (*miR-148b*, *miR-181b*, and *miR-874*) miRNAs for normalization. Multiple reference genes for RNA RT-PCR normalization are recommended over single reference genes (Bustin, 2002, Tricarico et al., 2002). Genetic mutations in the examined UCC lines might explain why primers for *miRNAs 29a*, *874*, *148b*, *539* and *524* were not able to give results in the respective experiments.

Assuming correct handling of probes and reagents, epigenetic silencing of certain miRNAs in these UCC is also possible mechanism explaining lack of results in primer efficiency testing. A possible link between epigenetic silencing of miRNAs and development of bladder cancer has been established previously (Shimizu et al., 2013).

Overall, spike-in controls may serve as an alternative normalization method in miRNA quantification in UCC cell lines. Spike-in controls have proven to provide a useful tool for process control, as the copy number can be spiked with a known amount and they do not display a significant cross-reactivity with any human miRNA (Redshaw et al., 2013). An increased amount of genetic material in the cDNA pool from UCC cell lines might also yield more consistent results. These factors must be considered in future miRNA qRT-PCRs.

4.4 miRNAs as Tumor Suppressors in UCC Lines

MiRNA expression levels were examined in UCC lines *UC 6*, *UC 16*, *5637*, *Cal-29*, *TCC*, *253J* and *HT1197*. These cell lines were chosen according to their CD276 protein expression, as miRNAs presumably have the highest regulatory impact on this level of expression. Previous studies showed *UC 6* and *UC 16* expressing low level of CD276 protein compared to somatic urothelial cells. *5637* and *Cal-29* represent a group of cells expressing moderate protein levels of CD276. *TCC* was chosen as a well-established UCC reference cell line with a moderate to high CD276 protein expression. *253J* and *HT1197* were UCC cell lines with the highest level of CD276 protein expression (unpublished results of research group of Prof. Dr. Aicher, not shown).

4.4.1 miRNA 29c

The results show that in some UCC lines *miRNA 29c* seems to be downregulated, while in others, expression is not affected or even upregulated. Upregulation of miRNAs in UCC is not uncommon, in fact, the first discovery of altered miRNA expression in UCC included upregulation of over 10 miRNAs (Gottardo et al., 2007). Low expression of *miRNA 29c* is associated with decreased progression-free-survival and has been found to be downregulated about 2-fold in progressing tumors (Dyrskjøt et al., 2009). This downregulation can be confirmed in cell lines *UC 6*, *Cal-29* and *HT1197*. Upregulation and

strongly varying results in other cell lines raises the question of other up- or downstream changes for *miRNA 29c*.

Different mechanisms for the role of *miRNA 29c* downregulation in tumor progression and carcinogenesis have been proposed. *CDK6* is a direct target of *miRNA 29c* in bladder cancer and regulates cell growth and invasion (Zhao et al., 2015). It was also found to be involved in the *PI3K/AKT* signaling pathway regulating apoptosis (Fan et al., 2014). In other types of cancer, multiple targets have been identified (DNMT3A, DNMT3B, p85alpha, CDC42, Bcl-2, Mcl-1, CCND2, and E2F7) (Morita et al., 2013, Park et al., 2009, Li et al., 2012).

In cell line *HT1197*, it can be assumed that *miRNA 29c* plays a major role in regulation of CD276 protein expression. As shown in Figure 26, downregulation of *miRNA 29c* leads to overexpression of CD276 and may therefore be a crucial factor in carcinogenesis and tumor progression in UCC. It may therefore function as a tumor suppressor. *Cal-29* results support this theory, although not as strongly. For further studies on *miRNA 29c* as a tumor suppressor in UCC, *HT1197* is highly suggested.

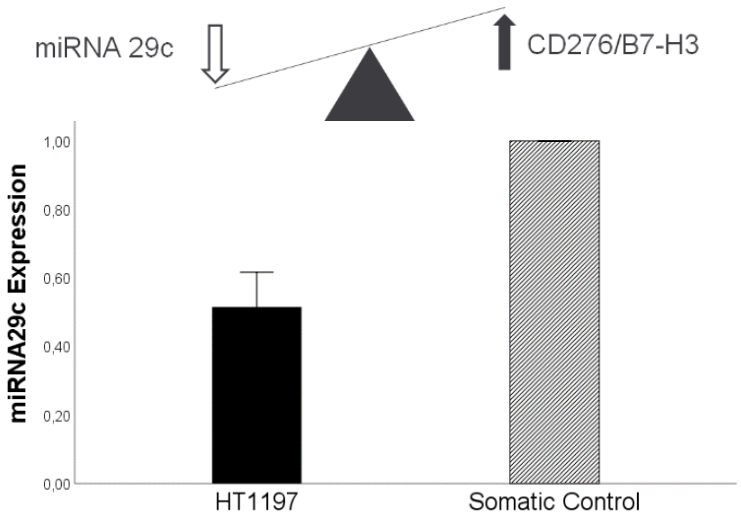

Figure 26: miRNA 29c as a tumor suppressor in cell line HT1197. Mean expression in cell line HT1197 compared to somatic urothelium and its effect on CD276 protein expression.

4.4.2 miRNA 187

The results of this work support the complex role of *miRNA 187* in tumors. It was found to be overexpressed in ovarian cancer and associated with a better prognosis (Chao et al., 2012). In other cancers such as ccRCC (clear cell Renal Cell Carcinoma), *miRNA 187* was found to be downregulated and proposed as a tumor suppressor by targeting CD276 (Zhao et al., 2013). In bladder cancer tissue, *miRNA 187-5p* was found to be upregulated and associated with higher risk of recurrence (Li et al., 2018b). These contrasting findings are also observed in this study, however *miRNA 187-3p* has been analyzed. A possible overexpression of CD276 by downregulation of *miRNA 187* cannot be clearly observed. Cell lines *UC 16*, *5637* and *253J* are cell lines expressing *miRNA 187* significantly lower and CD276 protein only moderately higher than somatic urothelium. CD276 as a direct target of *miRNA 187* must be viewed critically in bladder cancer. The role of *miRNA 187* as a tumor suppressor in bladder cancer cannot be confirmed according to this work. Up- or downregulation of *miRNA 187* may underly tissue specific mechanisms. Furthermore, miRNAs themselves are subject to a complex control. Regulation of miRNA gene transcription by transcription factors, miRNA processing and regulation of miRNA function are possible control mechanisms (Krol et al., 2010). Several of these control mechanisms might be altered in these UCC lines, as well. The exploration and detection of these mechanisms in urothelial carcinomas will have to be subject to future studies.

Overall, in different UCC lines different miRNAs appear to be the regulating factors for CD276. Tumor stage and progression play a major role in the extend of miRNA expression changes and should be accounted for. MiRNA expression may change throughout the process of tumorigenesis and progress, as some of its functions may be beneficial for the progress of tumor cells, while others may be harmful. For *HT1197*, results strongly suggest *miRNA 29c* as a regulator of CD276. To understand, if miRNAs are a possible therapeutic concept or clinical biomarker, tumor samples should be further sub-classified. This work confirms that tumors are a heterogenous construct rather than a uniform group of cells.

Molecular classification and sub-division of tumor cells will be necessary to effectively interpret biomarkers such as miRNAs or molecules like CD276.

4.5 Conclusion

In contrast to other UCC lines investigated previously (e.g., HT1197, Cal 29 and others) this study provided evidence that the expression of CD276 in most of the UCC lines investigated here (urothelial carcinoma UC5 to UC16), is not elevated in relation to somatic urothelial cells. However, proliferation rates of analyzed UCC lines were significantly higher than those of somatic urothelium. The inverse correlation between cell proliferation and CD276 mRNA expression may be a marker for tumor stem cells. Tumor stem cells generally have a lower proliferation rate and CD276 expression may therefore indicate tumor stem cell origin (Rossi 2020). Growth morphology showed UCC lines mostly growing in a cluster-like formation with some UCC growing more loosely. These findings suggest different stages of epithelial-mesenchymal transition (EMT) in different UCC cell lines.

Results of CD276 mRNA expression revealed a low median expression in analyzed UCC lines, with only cell line *UC 10* expressing CD276 mRNA higher than somatic urothelium. Overall CD276 protein levels were slightly lower in UCC lines compared to urothelium. Only three UCC lines had protein levels higher than somatic urothelium. However, on the cell surface of analyzed UCC lines, CD276 expression was higher than that of somatic urothelium. This provides further evidence for the complex regulation of this molecule. CD276 as a clinical biomarker has therefore to be viewed critically and anti-CD276 therapy should aim at cell surface expression to achieve maximal effects.

CD276 mRNA expression correlated moderately with CD276 protein expression and strongly with CD276 surface expression. Duplication rate of cell lines correlated inversely with CD276 mRNA and protein expression. Further regulation of CD276 transcription and translation by unknown factors must be

assumed. Cell surface receptor recycling may play a major role in the expression levels of CD276.

In UCC lines expressing CD276 protein on low, moderate or high levels, miRNA expression was analyzed. For *miRNA 29c* a regulatory role of CD276 in bladder cancer can be assumed, especially in cell line *HT1197*. It may function as a tumor suppressor by decreasing CD276 expression. The complex role of *miRNA 187* seen in other tumors could be observed in this work, as well. CD276 may only be an indirect target for regulation by *miRNA 187*, other factors must be considered in the regulation of CD276 by *miRNA 187* in bladder cancer.

Drawing these conclusions may help understanding the complex regulation of CD276 on a cellular level. Results underline the heterogenous character of UC and recommend a molecular sub-classification in patients for optimal treatment. An individual approach to each patient based on a variety of genetic markers may be able to give better treatment options and therapeutic success in the future.

5 Summary

Bladder cancer ranks among the 10 most common forms of cancer and is responsible for approximately 200,000 deaths annually. Between 90 to 95% of bladder cancers consists of urothelial carcinoma cells. A variety of features are characteristic for these tumor cells. One of these features is the evasion of the immune system. CD276 alias B7-H3 is a molecule from the superfamily of immune checkpoint molecules, which is suspected to have a co-inhibitory effect on the anti-tumor response and thereby helping tumor cells in the evasion of the immune system. It is overexpressed in a variety of different cancers, including bladder cancer and is associated with a poor prognosis and decreased overall survival. Furthermore, CD276 expression is believed to be regulated by miRNAs. *MiRNA 29c* and *miRNA 187* may act as tumor suppressors by decreasing CD276 expression in cells.

The aim of this work was to quantify expression levels of CD276 in urothelial carcinoma cell lines *UC 5, UC 6*, *UC 9*, *UC 10*, *UC 13*, *UC 14*, *UC 15* and *UC 16* in comparison to somatic urothelial cells. Furthermore, expression levels of *miRNA 29c* and *miRNA 187* were analyzed in selected UCC lines to confirm their regulatory role in UCC. The cells were examined for growth pattern and proliferation. Measurement of CD276 mRNA levels was executed by qRT-PCR. To quantify CD276 protein expression, an SDS-gel-electrophoresis followed by a Western Blot was performed. Expression of CD276 on the cell surface was observed by flow cytometry. To understand the regulation of CD276 expression by miRNAs, urothelial carcinoma cell lines *UC 6*, *UC 16*, *Cal-29*, *5637*, *TCC*, *253J* and *HT1176* were chosen according to low, moderate and high CD276 protein expression. In these cell lines, expression levels of *miRNA 29c* and *miRNA 187* were quantified by qRT-PCR. Possible *Mycoplasma* contaminations of cell cultures have been tested for and ruled out. Results of proliferation and growth pattern data revealed a higher proliferation rate in all UCC cell lines compared to somatic cells. UCC cells were mostly growing in a tight cluster-like

formation, while somatic cells formed loose colonies. CD276 mRNA expression analysis revealed a low median expression in analyzed UCC cell lines, with only cell line *UC 10* expressing CD276 mRNA higher than somatic urothelium. CD276 protein expression was highest in UCC line *UC 5* with around twice as much as in somatic. Other UCC lines expressed CD276 protein moderately or low. In all UCC lines except *UC 13*, surface expression of CD276 was higher than on somatic urothelial cells. In order to quantify miRNA expression in selected UCC lines, target and reference genes had to be established. M*iRNA 29c* and *miRNA 187* were established as target genes, *SNORD49a* and *miRNA 181b* were established as reference genes. Results showed downregulation of *miRNA 29c* in UCC line *HT1197* and *Cal-29*. Overall expression of *miRNA 29c* in analyzed UCC lines was significantly decreased. In UCC lines *UC 16*, *5637* and *253J*, *miRNA 187* expression was significantly decreased. Duplication rate correlated negatively with CD276 mRNA and protein expression. CD276 mRNA expression correlated moderately with CD276 protein expression and strongly with CD276 surface-expression.

Different growth patterns of UCC lines may result from uneven progression in Epithelial-Mesenchymal-Transition (EMT), as CD276 overexpression correlates with low E-cadherin expression. Because of its variable expression in UCC lines, CD276 mRNA expression as a biomarker for bladder cancer must be viewed critically. Furthermore, analyzed UCC lines may have formed sub-clones with different genetic expressions, while undergoing passaging. The lack of clear linear correlations between CD276 mRNA, protein and cell surface expression is most likely due to complex regulatory mechanisms. Regulatory mechanisms for CD276 include regulation by miRNAs. In UCC lines *HT1197* and *Cal-29*, *miRNA 29c* expression was downregulated. Downregulation of *miRNA 29c* leads to overexpression of CD276 and may therefore be a crucial factor in tumor progression and immune evasion of UCC. On the other hand, a possible overexpression of CD276 by downregulation of *miRNA 187* cannot be clearly observed. Results of this work underline the heterogenous character of UCC and recommend a molecular sub-classification in patients for optimal treatment.

6 German Summary

Das Blasenkarzinom ist eines der 10 häufigsten Krebsarten weltweit und ist verantwortlich für bis zu 200 000 Todesfälle jährlich. Zwischen 90 und 95% dieser Blasenkarzinome sind Urothelkarzinome. Eine Reihe von Merkmalen zeigt sich charakteristisch für diese Tumore. Eines dieser Merkmale ist die Fähigkeit, sich dem körpereigenen Immunsystem zu entziehen. CD276 alias B7-H3 ist ein Molekül aus der Superfamilie der Immune-Checkpoint-Moleküle und steht im Verdacht durch einen Co-Inhibitionseffekt auf die Anti-Tumor-Antwort es Tumorzellen zu ermöglichen, sich dem Immunsystem zu entziehen. CD276 wird in einer Reihe von Tumoren überexprimiert, darunter Blasenkrebs, und ist mit einer schlechteren Prognose und einem geringen Gesamtüberleben assoziiert. MiRNAs stehen im Verdacht, die Expression von CD276 zu steuern. *MiRNA 29c* und *miRNA 187* könnten hierbei als Tumorsuppressoren die Expression von CD276 vermindern. Ziel dieser Arbeit war es, die Expression von CD276 in Urothelkarzinom-Zelllinien UC 5, UC 6, UC 9, UC 10, UC 13, UC 14, UC 15 und UC 16 zu untersuchen. Des Weiteren wurde die Regulation der Expression von CD276 durch *miRNA 29c* und *miRNA 187* in ausgewählten Urothelkarzinom-Zelllinien untersucht. Die Zellen wurden auf ihr Wachstumsverhalten und ihre Proliferationsgeschwindigkeit hin untersucht. Die Expression von CD276 mRNA wurde durch ein qRT-PCR quantifiziert. Die Expressionslevel von CD276 auf Proteinebene wurden durch eine SDS-Gelelektrophorese gefolgt von einem Western-Blot analysiert. Zur Quantifizierung der Expression von CD276 an der Zelloberfläche wurde eine Flow-Zytometrie durchgeführt. Um die Regulation von CD276 durch miRNAs zu untersuchen, wurden UCC Zelllinien *UC 6, UC 16, Cal-29, 5637, TCC, 253J* und *HT1176* anhand niedriger, moderater und hoher Expression von CD276 Protein ausgewählt und mittels qRT-PCR analysiert. Alle Zellkulturen wurden auf eine mögliche Kontamination durch *Mykoplasmen* überprüft. Die Ergebnisse der Wachstumsanalyse und Proliferationsraten zeigte eine schnellere Proliferation in UC Zellen im Vergleich zu somatischen Zellen. UC Zellen

wuchsen meist in engen Cluster-Formationen, während somatische Zellen eher lose Kolonien formten. Die CD276 mRNA Expression zeigte sich in allen UC Zelllinien, außer UC 10, gleich oder niedriger als in somatischem Urothel. Die CD276 Proteinexpression war in Zellline UC 5 ungefähr doppelt so hoch, wie in somatischem Urothel, in den anderen Zelllinien moderat bis niedrig. An der Zelloberfläche wurde CD276 auf fast allen Zelllinien höher exprimiert als auf somatischen Urothelzellen. Zur Analyse einer potenziellen Regulation der Expression durch miRNAs konnten miRNA 29c und miRNA 187 als Zielgene, sowie SNORD49a und miRNA 181b als Referenzgene etabliert werden. In UC Zelllinien HT1197 und Cal-29 zeigte sich eine verminderte Expression von miRNA29c. Die Gesamtexpression von von miRNA 29c in den UC Zelllinien ziegte sich ebenfalls signifikant vermindert. In UC Zelllinien UC 16, 5637 und 253J zeigte sich die miRNA 187 expression signifikant niedriger. Die Korrelationsanalyse ergab eine negative Korrelation der Proliferationsgeschwindigkeit mit CD276 mRNA und Protein Expression. CD276 mRNA Expression korrelierte moderat mit der Proteinexpression und stark mit der Expression von CD276 an der Zelloberfläche. Die verschiedenen Wachstumsmuster der UC Zelllinien könnte durch ein uneinheitliches Fortschreiten der EMT bedingt sein, da die Überexpression von CD276 mit niedriger E-cadherin Expression korreliert. Aufgrund der variablen Expressionslevel muss die Expression von CD276 mRNA als klinischer Biomarker kritisch beurteilt werden. Jedoch könnten sich in den Zellkulturen aufgrund des häufigen Passagierens auch genetische Sub-Klone gebildet haben. Das Fehlen einer klaren, linearen Korrelation von CD276 mRNA-, Protein- und Zelloberflächenexpression deutet auf eine komplexe Regulation des Moleküls durch z.B. miRNAs hin. In den Zelllinien HT1197 und Cal-29 kann diese Regulation durch eine verminderte Expression von miRNA29c bestätigt werden und könnte somit ein entscheidender Faktor in der Tumorprogression des UC sein. Bei miRNA 187 bestätigt sich die unklare Rolle, welche in anderen Tumoren beobachtet wurde. Die Ergebnisse dieser Arbeit unterstreichen den heterogenen Charakter des UC und zeigen die Wichtigkeit einer molekularen Sub-Klassifikation von Patienten für deren optimale Therapie.

7 Bibliography

ABERN, M. R., DUDE, A. M., TSIVIAN, M. & COOGAN, C. L. 2013. The characteristics of bladder cancer after radiotherapy for prostate cancer. *Urologic Oncology: Seminars and Original Investigations,* 31**,** 1628-1634.

AICHER, W. K., KORN, M., REITNAUER, L., MAURER, F. B., HENNENLOTTER, J., BLACK, P. C., TODENHOFER, T., BEDKE, J. & STENZL, A. 2021. Expression patterns of the immune checkpoint ligand CD276 in urothelial carcinoma. *BMC Urology,* 21**,** 60.

AMBROS, V. 2004. The functions of animal microRNAs. *Nature,* 431**,** 350-355.

ANTONI, S., FERLAY, J., SOERJOMATARAM, I., ZNAOR, A., JEMAL, A. & BRAY, F. 2017. Bladder Cancer Incidence and Mortality: A Global Overview and Recent Trends. *European Urology,* 71**,** 96-108.

BARTEL, D. P. 2009. MicroRNAs: Target Recognition and Regulatory Functions. *Cell,* 136**,** 215-233.

BELLMUNT, J., DE WIT, R., VAUGHN, D. J., FRADET, Y., LEE, J.-L., FONG, L., VOGELZANG, N. J., CLIMENT, M. A., PETRYLAK, D. P., CHOUEIRI, T. K., NECCHI, A., GERRITSEN, W., GURNEY, H., QUINN, D. I., CULINE, S., STERNBERG, C. N., MAI, Y., POEHLEIN, C. H., PERINI, R. F. & BAJORIN, D. F. 2017. Pembrolizumab as Second-Line Therapy for Advanced Urothelial Carcinoma. *New England Journal of Medicine,* 376**,** 1015-1026.

BIEBACK, K., KERN, S., KLÜTER, H. & EICHLER, H. 2004. Critical parameters for the isolation of mesenchymal stem cells from umbilical cord blood. *Stem Cells,* 22**,** 625-34.

BILLEREY, C., CHOPIN, D., AUBRIOT-LORTON, M. H., RICOL, D., GIL DIEZ DE MEDINA, S., VAN RHIJN, B., BRALET, M. P., LEFRERE-BELDA, M. A., LAHAYE, J. B., ABBOU, C. C., BONAVENTURE, J., ZAFRANI, E. S., VAN DER KWAST, T., THIERY, J. P. & RADVANYI, F. 2001. Frequent FGFR3 mutations in papillary non-invasive bladder (pTa) tumors. *The American Journal of Pathology,* 158**,** 1955-1959.

BRAY, F., FERLAY, J., SOERJOMATARAM, I., SIEGEL, R. L., TORRE, L. A. & JEMAL, A. 2018. Global cancer statistics 2018: GLOBOCAN estimates of incidence and mortality worldwide for 36 cancers in 185 countries. *CA: A Cancer Journal for Clinicians* 2018 Nov;68(6):394-424.

BRUYNINCKX, R., BUNTINX, F., AERTGEERTS, B. & VAN CASTEREN, V. 2003. The diagnostic value of macroscopic haematuria for the diagnosis of urological cancer in general practice. *The British Journal of General Practice : the Journal of the Royal College of General Practitioners,* 53**,** 31-35.

BURGER, M., CATTO, J. W. F., DALBAGNI, G., GROSSMAN, H. B., HERR, H., KARAKIEWICZ, P., KASSOUF, W., KIEMENEY, L. A., LA VECCHIA,

C., SHARIAT, S. & LOTAN, Y. 2013. Epidemiology and Risk Factors of Urothelial Bladder Cancer. *European Urology,* 63**,** 234-241.

BURR, M. L., SPARBIER, C. E., CHAN, Y. C., WILLIAMSON, J. C., WOODS, K., BEAVIS, P. A., LAM, E. Y. N., HENDERSON, M. A., BELL, C. C., STOLZENBURG, S., GILAN, O., BLOOR, S., NOORI, T., MORGENS, D. W., BASSIK, M. C., NEESON, P. J., BEHREN, A., DARCY, P. K., DAWSON, S. J., VOSKOBOINIK, I., TRAPANI, J. A., CEBON, J., LEHNER, P. J. & DAWSON, M. A. 2017. CMTM6 maintains the expression of PD-L1 and regulates anti-tumour immunity. *Nature,* 549**,** 101-105.

BUSTIN, S. A. 2002. Quantification of mRNA using real-time reverse transcription PCR (RT-PCR): trends and problems. *Journal of Molecular Endocrinology,* 29**,** 23-39.

CALIN, G. A., DUMITRU, C. D., SHIMIZU, M., BICHI, R., ZUPO, S., NOCH, E., ALDLER, H., RATTAN, S., KEATING, M., RAI, K., RASSENTI, L., KIPPS, T., NEGRINI, M., BULLRICH, F. & CROCE, C. M. 2002. Frequent deletions and down-regulation of micro- RNA genes miR15 and miR16 at 13q14 in chronic lymphocytic leukemia. *Proceedings of the National Academy of Sciences U S A,* 99**,** 15524-15529.

CAPES-DAVIS, A., THEODOSOPOULOS, G., ATKIN, I., DREXLER, H. G., KOHARA, A., MACLEOD, R. A. F., MASTERS, J. R., NAKAMURA, Y., REID, Y. A., REDDEL, R. R. & FRESHNEY, R. I. 2010. Check your cultures! A list of cross-contaminated or misidentified cell lines. *International Journal of Cancer,* 127**,** 1-8.

CASTELLANOS, J. R., PURVIS, I. J., LABAK, C. M., GUDA, M. R., TSUNG, A. J., VELPULA, K. K. & ASUTHKAR, S. 2017. B7-H3 role in the immune landscape of cancer. *American Journal of Clininical and Experimental Immunology,* 6**,** 66-75.

CATTAN, N., ROCHET, N., MAZEAU, C., ZANGHELLINI, E., MARI, B., CHAUZY, C., NOVION, H. S. D., AMIEL, J., LAGRANGE, J. L., ROSSI, B. & GIOANNI, J. 2001. Establishment of two new human bladder carcinoma cell lines, CAL 29 and CAL 185. Comparative study of cell scattering and epithelial to mesenchyme transition induced by growth factors. *British Journal of Cancer,* 85**,** 1412-1417.

CATTO, J. W. F., ALCARAZ, A., BJARTELL, A. S., DE VERE WHITE, R., EVANS, C. P., FUSSEL, S., HAMDY, F. C., KALLIONIEMI, O., MENGUAL, L., SCHLOMM, T. & VISAKORPI, T. 2011. MicroRNA in Prostate, Bladder, and Kidney Cancer: A Systematic Review. *European Urology,* 59**,** 671-681.

CATTO, J. W. F., HARTMANN, A., STOEHR, R., BOLDERSON, E., REHMAN, I., ROSARIO, D. J., HAMDY, F. C. & MEUTH, M. 2006. Multifocal Urothelial Cancers With the Mutator Phenotype are of Monoclonal Origin and Require Panurothelial Treatment for Tumor Clearance. *The Journal of Urology,* 175**,** 2323-2330.

CHAMES, P., VAN REGENMORTEL, M., WEISS, E. & BATY, D. 2009. Therapeutic antibodies: successes, limitations and hopes for the future. *British Journal of Pharmacology,* 157**,** 220-233.

CHANG, S. S., BOORJIAN, S. A., CHOU, R., CLARK, P. E., DANESHMAND, S., KONETY, B. R., PRUTHI, R., QUALE, D. Z., RITCH, C. R., SEIGNE, J. D., SKINNER, E. C., SMITH, N. D. & MCKIERNAN, J. M. 2016. Diagnosis and Treatment of Non-Muscle Invasive Bladder Cancer: AUA/SUO Guideline.*The Journal of Urology,* 196**,** 1021-9.

CHAO, A., LIN, C. Y., LEE, Y. S., TSAI, C. L., WEI, P. C., HSUEH, S., WU, T. I., TSAI, C. N., WANG, C. J., CHAO, A. S., WANG, T. H. & LAI, C. H. 2012. Regulation of ovarian cancer progression by microRNA-187 through targeting Disabled homolog-2. *Oncogene,* 31**,** 764-775.

CHAPOVAL, A. I., NI, J., LAU, J. S., WILCOX, R. A., FLIES, D. B., LIU, D., DONG, H., SICA, G. L., ZHU, G., TAMADA, K. & CHEN, L. 2001. B7-H3: A costimulatory molecule for T cell activation and IFN-γ production. *Nature Immunology,* 2**,** 269.

CHEN, Z.-R., ZHANG, G.-B., WANG, Y.-Q., YAN, Y.-D., ZHOU, W.-F., ZHU, C.-H., WANG, J. & JI, W. 2013. Soluble B7-H3 elevations in hospitalized children with Mycoplasma pneumoniae pneumonia. *Diagnostic Microbiology and Infectious Disease,* 77**,** 362-366.

CUMBERBATCH, M. G. K., JUBBER, I., BLACK, P. C., ESPERTO, F., FIGUEROA, J. D., KAMAT, A. M., KIEMENEY, L., LOTAN, Y., PANG, K., SILVERMAN, D. T., ZNAOR, A. & CATTO, J. W. F. 2018. Epidemiology of Bladder Cancer: A Systematic Review and Contemporary Update of Risk Factors in 2018. *European Urology,* 74(6), 784-795.

DONG, P., XIONG, Y., YUE, J., HANLEY, S. J. B. & WATARI, H. 2018. B7H3 As a Promoter of Metastasis and Promising Therapeutic Target. 8.

DYRSKJØT, L., OSTENFELD, M. S., BRAMSEN, J. B., SILAHTAROGLU, A. N., LAMY, P., RAMANATHAN, R., FRISTRUP, N., JENSEN, J. L., ANDERSEN, C. L., ZIEGER, K., KAUPPINEN, S., ULHØI, B. P., KJEMS, J., BORRE, M. & ORNTOFT, T. F. 2009. Genomic profiling of microRNAs in bladder cancer: miR-129 is associated with poor outcome and promotes cell death in vitro. *Cancer Research,* 69**,** 4851-60.

ELLIOTT, A. Y., CLEVELAND, P., CERVENKA, J., CASTRO, A. E., STEIN, N., HAKALA, T. R. & FRALEY, E. E. 1974. Characterization of a cell line from human transitional cell cancer of the urinary tract. *Journal of the National Cancer Institute,* 53**,** 1341-9.

FABIAN, M. R., SONENBERG, N. & FILIPOWICZ, W. 2010. Regulation of mRNA Translation and Stability by microRNAs. *Annual Review of Biochemistry,* 79**,** 351-379.

FAN, Y., SONG, X., DU, H., LUO, C., WANG, X., YANG, X., WANG, Y. & WU, X. 2014. Down-regulation of miR-29c in human bladder cancer and the inhibition of proliferation in T24 cell via PI3K-AKT pathway. *Medical Oncology,* 31**,** 65.

FARAZI, T. A., SPITZER, J. I., MOROZOV, P. & TUSCHL, T. 2011. miRNAs in human cancer. *The Journal of Pathology,* 223**,** 102-115.

FLEM-KARLSEN, K., FODSTAD, Ø., TAN, M. & NUNES-XAVIER, C. E. 2018. B7-H3 in Cancer – Beyond Immune Regulation. *Trends in Cancer,* 4**,** 401-404.

FOGH, J. M., FOGH, J. & ORFEO, T. 1977. One Hundred and Twenty-Seven Cultured Human Tumor Cell Lines Producing Tumors in Nude Mice23. *JNCI: Journal of the National Cancer Institute,* 59**,** 221-226.

FULLER, T. W., ACHARYA, A. P., MEYYAPPAN, T., YU, M., BHASKAR, G., LITTLE, S. R. & TARIN, T. V. 2018. Comparison of Bladder Carcinogens in the Urine of E-cigarette Users Versus Non E-cigarette Using Controls. *Scientific Reports,* 8**,** 507.

GABRIEL, U., LI, L., BOLENZ, C., STEIDLER, A., KRÄNZLIN, B., SAILE, M., GRETZ, N., TROJAN, L. & MICHEL, M. S. 2012. New insights into the influence of cigarette smoking on urothelial carcinogenesis: Smoking-induced gene expression in tumor-free urothelium might discriminate muscle-invasive from nonmuscle-invasive urothelial bladder cancer. *Molecular Carcinogenesis,* 51**,** 907-915.

GOTTARDO, F., LIU, C. G., FERRACIN, M., CALIN, G. A., FASSAN, M., BASSI, P., SEVIGNANI, C., BYRNE, D., NEGRINI, M., PAGANO, F., GOMELLA, L. G., CROCE, C. M. & BAFFA, R. 2007. Micro-RNA profiling in kidney and bladder cancers. *Urologic Oncology: Seminars and Original Investigations,* 25**,** 387-392.

GROSSMAN, H. B., WEDEMEYER, G., REN, L., WILSON, G. N. & COX, B. 1986. Improved Growth of Human Urothelial Carcinoma Cell Cultures. *The Journal of Urology*,136**,** 953-959.

HAMMOND, S. M. 2006. RNAi, microRNAs, and human disease. *Cancer Chemotherapy and Pharmacology,* 58**,** 63-68.

HANAHAN, D. & WEINBERG, R. A. 2011. Hallmarks of cancer: the next generation. *Cell,* 144**,** 646-74.

HASHIGUCHI, M. 2012. Human B7-H3 binds to Triggering receptor expressed on myeloid cells-like transcript 2 (TLT-2) and enhances T cell responses. *Open Journal of Immunology,* 02**,** 9-16.

HUMPHREY, P. A., MOCH, H., CUBILLA, A. L., ULBRIGHT, T. M. & REUTER, V. E. 2016. The 2016 WHO Classification of Tumours of the Urinary System and Male Genital Organs-Part B: Prostate and Bladder Tumours. *European Urology,* 70**,** 106-119.

IWAI, Y., ISHIDA, M., TANAKA, Y., OKAZAKI, T., HONJO, T. & MINATO, N. 2002. Involvement of PD-L1 on tumor cells in the escape from host immune system and tumor immunotherapy by PD-L1 blockade. *Proceedings of the National Academy of Sciences of the United States of America U S A,* 99**,** 12293-7.

JANAKIRAM, M., SHAH, U. A., LIU, W., ZHAO, A., SCHOENBERG, M. P. & ZANG, X. 2017. The third group of the B7-CD28 immune checkpoint family: HHLA2, TMIGD2, B7x, and B7-H3. *Immunological Reviews,* 276**,** 26-39.

JIANG, B., LIU, F., LIU, Z., ZHANG, T. & HUA, D. 2016a. B7-H3 increases thymidylate synthase expression via the PI3k-Akt pathway. *Tumor Biology,* 37**,** 9465-72.

JIANG, B., ZHANG, T., LIU, F., SUN, Z., SHI, H., HUA, D. & YANG, C. 2016b. The co-stimulatory molecule B7-H3 promotes the epithelial-mesenchymal transition in colorectal cancer. *Oncotarget,* 7**,** 31755-31771.

KAMAT, A. M., HAHN, N. M., EFSTATHIOU, J. A., LERNER, S. P., MALMSTRÖM, P.-U., CHOI, W., GUO, C. C., LOTAN, Y. & KASSOUF, W. 2016. Bladder cancer. *The Lancet,* 388**,** 2796-2810.

KAUR, G. & DUFOUR, J. M. 2012. Cell lines: Valuable tools or useless artifacts. *Spermatogenesis,* 2**,** 1-5.

KIM, V. N. 2005. MicroRNA biogenesis: coordinated cropping and dicing. *Nature Reviews Molecular Cell Biology,* 6**,** 376-385.

KROL, J., LOEDIGE, I. & FILIPOWICZ, W. 2010. The widespread regulation of microRNA biogenesis, function and decay. *Nature Reviews Genetics,* 11**,** 597-610.

LEE, R. C., FEINBAUM, R. L. & AMBROS, V. 1993. The C. elegans heterochronic gene lin-4 encodes small RNAs with antisense complementarity to lin-14. *Cell,* 75**,** 843-54.

LEITNER, J., KLAUSER, C., PICKL, W. F., STOCKL, J., MAJDIC, O., BARDET, A. F., KREIL, D. P., DONG, C., YAMAZAKI, T., ZLABINGER, G., PFISTERSHAMMER, K. & STEINBERGER, P. 2009. B7-H3 is a potent inhibitor of human T-cell activation: No evidence for B7-H3 and TREML2 interaction. *European Journal of Immunology,* 39**,** 1754-64.

LEUNG, J. & SUH, W.-K. 2014. The CD28-B7 Family in Anti-Tumor Immunity: Emerging Concepts in Cancer Immunotherapy. *Immune Network,* 14**,** 265-276.

LI, G., QUAN, Y., CHE, F. & WANG, L. 2018a. B7-H3 in tumors: friend or foe for tumor immunity? *Cancer Chemotherapy and Pharmacology,* 81**,** 245-253.

LI, L., SARVER, A. L., ALAMGIR, S. & SUBRAMANIAN, S. 2012. Downregulation of microRNAs miR-1, -206 and -29 stabilizes PAX3 and CCND2 expression in rhabdomyosarcoma. *Laboratory Investigation,* 92**,** 571-83.

LI, Y., GUO, G., SONG, J., CAI, Z., YANG, J., CHEN, Z., WANG, Y., HUANG, Y. & GAO, Q. 2017. B7-H3 Promotes the Migration and Invasion of Human Bladder Cancer Cells via the PI3K/Akt/STAT3 Signaling Pathway. *Journal of Cancer,* 8**,** 816-824.

LI, Z., LIN, C., ZHAO, L., ZHOU, L., PAN, X., QUAN, J., PENG, X., LI, W., LI, H., XU, J., XU, W., GUAN, X., CHEN, Y. & LAI, Y. 2018b. Oncogene miR-187-5p is associated with cellular proliferation, migration, invasion, apoptosis and an increased risk of recurrence in bladder cancer. *Biomedicine & Pharmacotherapy,* 105**,** 461-469.

LIM, S., LIU, H., MADEIRA DA SILVA, L., ARORA, R., LIU, Z., PHILLIPS, J. B., SCHMITT, D. C., VU, T., MCCLELLAN, S., LIN, Y., LIN, W., PIAZZA, G. A., FODSTAD, O. & TAN, M. 2016. Immunoregulatory Protein B7-H3 Reprograms Glucose Metabolism in Cancer Cells by ROS-Mediated Stabilization of HIF1alpha. *Cancer Research,* 76**,** 2231-42.

LOO, D., ALDERSON, R. F., CHEN, F. Z., HUANG, L., ZHANG, W., GORLATOV, S., BURKE, S., CICCARONE, V., LI, H., YANG, Y., SON, T., CHEN, Y., EASTON, A. N., LI, J. C., RILLEMA, J. R., LICEA, M., FIEGER, C., LIANG, T. W., MATHER, J. P., KOENIG, S., STEWART, S. J., JOHNSON, S., BONVINI, E. & MOORE, P. A. 2012. Development of

an Fc-enhanced anti-B7-H3 monoclonal antibody with potent antitumor activity. *Clinical Cancer Research,* 18**,** 3834-45.

LOOS, M., HEDDERICH, D. M., OTTENHAUSEN, M., GIESE, N. A., LASCHINGER, M., ESPOSITO, I., KLEEFF, J. & FRIESS, H. 2009. Expression of the costimulatory molecule B7-H3 is associated with prolonged survival in human pancreatic cancer. *BMC Cancer,* 9**,** 463.

MAMESSIER, E., BIRNBAUM, D. J., FINETTI, P., BIRNBAUM, D. & BERTUCCI, F. 2018. CMTM6 stabilizes PD-L1 expression and refines its prognostic value in tumors. *Annals of Translational Medicine,* 6**,** 54-54.

MATTICK, J. S. 2001. Non-coding RNAs: the architects of eukaryotic complexity. *EMBO reports,* 2**,** 986-991.

MENGUAL, L., LOZANO, J. J., INGELMO-TORRES, M., GAZQUEZ, C., RIBAL, M. J. & ALCARAZ, A. 2013. Using microRNA profiling in urine samples to develop a non-invasive test for bladder cancer. *International Journal of Cancer,* 133**,** 2631-2641.

MEZZADRA, R., SUN, C., JAE, L. T., GOMEZ-EERLAND, R., DE VRIES, E., WU, W., LOGTENBERG, M. E. W., SLAGTER, M., ROZEMAN, E. A., HOFLAND, I., BROEKS, A., HORLINGS, H. M., WESSELS, L. F. A., BLANK, C. U., XIAO, Y., HECK, A. J. R., BORST, J., BRUMMELKAMP, T. R. & SCHUMACHER, T. N. M. 2017. Identification of CMTM6 and CMTM4 as PD-L1 protein regulators. *Nature,* 549**,** 106-110.

MORITA, S., HORII, T., KIMURA, M., OCHIYA, T., TAJIMA, S. & HATADA, I. 2013. miR-29 represses the activities of DNA methyltransferases and DNA demethylases. *International Journal of Molecular Sciences,* 14**,** 14647-14658.

NAYAK, S. K., O'TOOLE, C. & PRICE, Z. H. 1977. A cell line from an anaplastic transitional cell carcinoma of human urinary bladder. *British Journal of Cancer,* 35**,** 142-151.

NYGREN, M. K., TEKLE, C., INGEBRIGTSEN, V. A. & FODSTAD, O. 2011. B7-H3 and its relevance in cancer; immunological and non-immunological perspectives. *Frontiers in Bioscience (Elite Edition),* 3**,** 989-93.

NYGREN, M. K., TEKLE, C., INGEBRIGTSEN, V. A., MAKELA, R., KROHN, M., AURE, M. R., NUNES-XAVIER, C. E., PERALA, M., TRAMM, T., ALSNER, J., OVERGAARD, J., NESLAND, J. M., BORGEN, E., BORRESEN-DALE, A. L., FODSTAD, O., SAHLBERG, K. K. & LEIVONEN, S. K. 2014. Identifying microRNAs regulating B7-H3 in breast cancer: the clinical impact of microRNA-29c. *British Journal of Cancer,* 110**,** 2072-80.

PARK, H.-S., PARK, W. S., BONDARUK, J., TANAKA, N., KATAYAMA, H., LEE, S., SPIESS, P. E., STEINBERG, J. R., WANG, Z., KATZ, R. L., DINNEY, C., ELIAS, K. J., LOTAN, Y., NAEEM, R. C., BAGGERLY, K., SEN, S., GROSSMAN, H. B. & CZERNIAK, B. 2008. Quantitation of Aurora Kinase A Gene Copy Number in Urine Sediments and Bladder Cancer Detection. *JNCI: Journal of the National Cancer Institute England,* 100**,** 1401-1411.

PARK, S. Y., LEE, J. H., HA, M., NAM, J. W. & KIM, V. N. 2009. miR-29 miRNAs activate p53 by targeting p85 alpha and CDC42. *Nature Structural & Molecular Biology,* 16**,** 23-9.

PEREIRA, D. M., RODRIGUES, P. M., BORRALHO, P. M. & RODRIGUES, C. M. P. 2013. Delivering the promise of miRNA cancer therapeutics. *Drug Discovery Today,* 18**,** 282-289.

PHAN, G. Q., YANG, J. C., SHERRY, R. M., HWU, P., TOPALIAN, S. L., SCHWARTZENTRUBER, D. J., RESTIFO, N. P., HAWORTH, L. R., SEIPP, C. A., FREEZER, L. J., MORTON, K. E., MAVROUKAKIS, S. A., DURAY, P. H., STEINBERG, S. M., ALLISON, J. P., DAVIS, T. A. & ROSENBERG, S. A. 2003. Cancer regression and autoimmunity induced by cytotoxic T lymphocyte-associated antigen 4 blockade in patients with metastatic melanoma. *Proceedings of the National Academy of Sciences of the United States of America U S A,* 100**,** 8372-7.

PIZON, M., SCHOTT, D. S., PACHMANN, U. & PACHMANN, K. 2018. B7-H3 on circulating epithelial tumor cells correlates with the proliferation marker, Ki-67, and may be associated with the aggressiveness of tumors in breast cancer patients. *International Journal of Oncology,* 53**,** 2289-2299.

POWDERLY, J., COTE, G., FLAHERTY, K., SZMULEWITZ, R. Z., RIBAS, A., WEBER, J., LOO, D., BAUGHMAN, J., CHEN, F., MOORE, P., BONVINI, E., VASSELLI, J., WIGGINTON, J., COHEN, R., BURRIS, H. & CHMIELOWSKI, B. 2015. Interim results of an ongoing Phase I, dose escalation study of MGA271 (Fc-optimized humanized anti-B7-H3 monoclonal antibody) in patients with refractory B7-H3-expressing neoplasms or neoplasms whose vasculature expresses B7-H3. *Journal for Immunotherapy of Cancer,* 3**,** O8-O8.

POWLES, T., O'DONNELL, P. H., MASSARD, C., ARKENAU, H.-T., FRIEDLANDER, T. W., HOIMES, C. J., LEE, J. L., ONG, M., SRIDHAR, S. S., VOGELZANG, N. J., FISHMAN, M. N., ZHANG, J., SRINIVAS, S., PARIKH, J., ANTAL, J., JIN, X., GUPTA, A. K., BEN, Y. & HAHN, N. M. 2017. Efficacy and Safety of Durvalumab in Locally Advanced or Metastatic Urothelial Carcinoma: Updated Results From a Phase 1/2 Open-label Study. *JAMA Oncology,* 3**,** e172411-e172411.

RANA, T. M. 2007. Illuminating the silence: understanding the structure and function of small RNAs. *Nature Reviews Molecular Cell Biology,* 8**,** 23-36.

RASHEED, S., GARDNER, M. B., RONGEY, R. W., NELSON-REES, W. A. & ARNSTEIN, P. 1977. Human bladder carcinoma: characterization of two new tumor cell lines and search for tumor viruses. *Journal of the National Cancer Institute, England,* 58**,** 881-90.

RATERT, N., MEYER, H. A., JUNG, M., MOLLENKOPF, H. J., WAGNER, I., MILLER, K., KILIC, E., ERBERSDOBLER, A., WEIKERT, S. & JUNG, K. 2012. Reference miRNAs for miRNAome analysis of urothelial carcinomas. *PLoS One,* 7**,** e39309.

RAYN, K. N., HALE, G. R., GRAVE, G. P.-L. & AGARWAL, P. K. 2018. New therapies in nonmuscle invasive bladder cancer treatment. *Indian Journal of Urology : IJU : Journal of the Urological Society of India,* 34**,** 11-19.

REDSHAW, N., WILKES, T., WHALE, A., COWEN, S., HUGGETT, J. & FOY, C. A. 2013. A comparison of miRNA isolation and RT-qPCR technologies and their effects on quantification accuracy and repeatability. *BioTechniques,* 54**,** 155-164.

REUTER, V. E. 2006. The pathology of bladder cancer. *Urology,* 67**,** 11-17.

ROSSI, F., NOREN, H., JOVE, R., BELJANSKI, V. & GRINNEMO, K.-H. 2020. Differences and similarities between cancer and somatic stem cells: therapeutic implications. *Stem Cell Research & Therapy,* 11**,** 489.

SABICHI, A., KEYHANI, A., TANAKA, N., DELACERDA, J., LEE, I. L., ZOU, C., ZHOU, J. H., BENEDICT, W. F. & GROSSMAN, H. B. 2006. Characterization of a panel of cell lines derived from urothelial neoplasms: genetic alterations, growth in vivo and the relationship of adenoviral mediated gene transfer to coxsackie adenovirus receptor expression. *The Journal of Urology,* 175**,** 1133-7.

SANLI, O., DOBRUCH, J., KNOWLES, M. A., BURGER, M., ALEMOZAFFAR, M., NIELSEN, M. E. & LOTAN, Y. 2017. Bladder cancer. *Nature Reviews Disease Primers,* 3**,** 17022.

SCHMITZ-DRÄGER, B. J., DROLLER, M., LOKESHWAR, V. B., LOTAN, Y., HUDSON, M. A., VAN RHIJN, B. W., MARBERGER, M. J., FRADET, Y., HEMSTREET, G. P., MALMSTROM, P. U., OGAWA, O., KARAKIEWICZ, P. I. & SHARIAT, S. F. 2015. Molecular Markers for Bladder Cancer Screening, Early Diagnosis, and Surveillance: The WHO/ICUD Consensus. *Urologia Internationalis,* 94**,** 1-24.

SEAMAN, S., ZHU, Z., SAHA, S., ZHANG, X. M., YANG, M. Y., HILTON, M. B., MORRIS, K., SZOT, C., MORRIS, H., SWING, D. A., TESSAROLLO, L., SMITH, S. W., DEGRADO, S., BORKIN, D., JAIN, N., SCHEIERMANN, J., FENG, Y., WANG, Y., LI, J., WELSCH, D., DECRESCENZO, G., CHAUDHARY, A., ZUDAIRE, E., KLARMANN, K. D., KELLER, J. R., DIMITROV, D. S. & ST CROIX, B. 2017. Eradication of Tumors through Simultaneous Ablation of CD276/B7-H3-Positive Tumor Cells and Tumor Vasculature. *Cancer Cell,* 31**,** 501-515 e8.

SHARIAT, S. F., KARAKIEWICZ, P. I., PALAPATTU, G. S., LOTAN, Y., ROGERS, C. G., AMIEL, G. E., VAZINA, A., GUPTA, A., BASTIAN, P. J., SAGALOWSKY, A. I., SCHOENBERG, M. P. & LERNER, S. P. 2006. Outcomes of radical cystectomy for transitional cell carcinoma of the bladder: a contemporary series from the Bladder Cancer Research Consortium. The *Journal of Urology,* 176**,** 2414-22; discussion 2422.

SHARMA, P., RETZ, M., SIEFKER-RADTKE, A., BARON, A., NECCHI, A., BEDKE, J., PLIMACK, E. R., VAENA, D., GRIMM, M.-O., BRACARDA, S., ARRANZ, J. Á., PAL, S., OHYAMA, C., SACI, A., QU, X., LAMBERT, A., KRISHNAN, S., AZRILEVICH, A. & GALSKY, M. D. 2017. Nivolumab in metastatic urothelial carcinoma after platinum therapy (CheckMate 275): a multicentre, single-arm, phase 2 trial. *The Lancet Oncology,* 18**,** 312-322.

SHIMIZU, T., SUZUKI, H., NOJIMA, M., KITAMURA, H., YAMAMOTO, E., MARUYAMA, R., ASHIDA, M., HATAHIRA, T., KAI, M., MASUMORI, N., TOKINO, T., IMAI, K., TSUKAMOTO, T. & TOYOTA, M. 2013.

Methylation of a Panel of MicroRNA Genes Is a Novel Biomarker for Detection of Bladder Cancer. *European Urology,* 63**,** 1091-1100.

SHINOHARA, N., LIEBERT, M., WEDEMEYER, G., CHANG, J. H. C. & GROSSMAN, H. B. 1993. Evaluation of Multiple Drug Resistance in Human Bladder Cancer Cell Lines. *The Journal of Urology,* 150**,** 505-509.

SHRUTI, K., SHREY, K. & VIBHA, R. 2011. Micro RNAs: Tiny sequences with enormous potential. *Biochemical and Biophysical Research Communications,* 407**,** 445-449.

STEINBERGER, P., MAJDIC, O., DERDAK, S. V., PFISTERSHAMMER, K., KIRCHBERGER, S., KLAUSER, C., ZLABINGER, G., PICKL, W. F., STOCKL, J. & KNAPP, W. 2004. Molecular characterization of human 4Ig-B7-H3, a member of the B7 family with four Ig-like domains. *Journal of Immunology,* 172**,** 2352-9.

SYLVESTER, R. J., VAN DER MEIJDEN, A. P. M., OOSTERLINCK, W., WITJES, J. A., BOUFFIOUX, C., DENIS, L., NEWLING, D. W. W. & KURTH, K. 2006. Predicting Recurrence and Progression in Individual Patients with Stage Ta T1 Bladder Cancer Using EORTC Risk Tables: A Combined Analysis of 2596 Patients from Seven EORTC Trials. *European Urology,* 49**,** 466-477.

TEKLE, C., NYGREN, M. K., CHEN, Y.-W., DYBSJORD, I., NESLAND, J. M., MÆLANDSMO, G. M. & FODSTAD, Ø. 2012. B7-H3 contributes to the metastatic capacity of melanoma cells by modulation of known metastasis-associated genes. *International Journal of Cancer,* 130**,** 2282-2290.

THOMPSON, D. B., SIREF, L. E., FELONEY, M. P., HAUKE, R. J. & AGRAWAL, D. K. 2015. Immunological basis in the pathogenesis and treatment of bladder cancer. *Expert Review of Clinical Immunology,* 11**,** 265-279.

TRICARICO, C., PINZANI, P., BIANCHI, S., PAGLIERANI, M., DISTANTE, V., PAZZAGLI, M., BUSTIN, S. A. & ORLANDO, C. 2002. Quantitative real-time reverse transcription polymerase chain reaction: normalization to rRNA or single housekeeping genes is inappropriate for human tissue biopsies. *Analytical Biochemistry,* 309**,** 293-300.

VALE, C. L. 2005. Neoadjuvant Chemotherapy in Invasive Bladder Cancer: Update of a Systematic Review and Meta-Analysis of Individual Patient Data: Advanced Bladder Cancer (ABC) Meta-analysis Collaboration. *European Urology,* 48**,** 202-206.

VAN DE PUTTE, E. E. F., BOSSCHIETER, J., VAN DER KWAST, T. H., BERTZ, S., DENZINGER, S., MANACH, Q., COMPERAT, E. M., BOORMANS, J. L., JEWETT, M. A. S., STOEHR, R., VAN LEENDERS, G., NIEUWENHUIJZEN, J. A., ZLOTTA, A. R., HENDRICKSEN, K., ROUPRET, M., OTTO, W., BURGER, M., HARTMANN, A. & VAN RHIJN, B. W. G. 2018. The World Health Organization 1973 classification system for grade is an important prognosticator in T1 non-muscle-invasive bladder cancer. *BJU International,* 122**,** 978-985.

VANDER HEIDEN, M. G., CANTLEY, L. C. & THOMPSON, C. B. 2009. Understanding the Warburg effect: the metabolic requirements of cell proliferation. *Science,* 324**,** 1029-33.

WANG, J., CHONG, K. K., NAKAMURA, Y., NGUYEN, L., HUANG, S. K., KUO, C., ZHANG, W., YU, H., MORTON, D. L. & HOON, D. S. B. 2013. B7-H3 Associated with Tumor Progression and Epigenetic Regulatory Activity in Cutaneous Melanoma. *Journal of Investigative Dermatology,* 133**,** 2050-2058.

WANG, Z. S., ZHONG, M., BIAN, Y. H., MU, Y. F., QIN, S. L., YU, M. H. & QIN, J. 2016. MicroRNA-187 inhibits tumor growth and invasion by directly targeting CD276 in colorectal cancer. *Oncotarget,* 7**,** 44266-44276.

WESTHOFF, E., WITJES, J. A., FLESHNER, N. E., LERNER, S. P., SHARIAT, S. F., STEINECK, G., KAMPMAN, E., KIEMENEY, L. A. & VRIELING, A. 2018. Body Mass Index, Diet-Related Factors, and Bladder Cancer Prognosis: A Systematic Review and Meta-Analysis. *Bladder Cancer,* 4**,** 91-112.

WU, C. P., JIANG, J. T., TAN, M., ZHU, Y. B., JI, M., XU, K. F., ZHAO, J. M., ZHANG, G. B. & ZHANG, X. G. 2006. Relationship between co-stimulatory molecule B7-H3 expression and gastric carcinoma histology and prognosis. *World Journal of Gastroenterology,* 12**,** 457-9.

XIE, C., LIU, D., CHEN, Q., YANG, C., WANG, B. & WU, H. 2016. Soluble B7-H3 promotes the invasion and metastasis of pancreatic carcinoma cells through the TLR4/NF-κB pathway. *Scientific Reports,* 6**,** 27528.

XU, H., CHEUNG, I. Y., GUO, H. F. & CHEUNG, N. K. 2009. MicroRNA miR-29 modulates expression of immunoinhibitory molecule B7-H3: potential implications for immune based therapy of human solid tumors. *Cancer Research,* 69**,** 6275-81.

XU, Z., WANG, L., TIAN, J., MAN, H., LI, P. & SHAN, B. 2018. High expression of B7-H3 and CD163 in cancer tissues indicates malignant clinicopathological status and poor prognosis of patients with urothelial cell carcinoma of the bladder. *Oncology Letters,* 15**,** 6519-6526.

XYLINAS, E., ROBINSON, B. D., KLUTH, L. A., VOLKMER, B. G., HAUTMANN, R., KUFER, R., ZERBIB, M., KWON, E., THOMPSON, R. H., BOORJIAN, S. A. & SHARIAT, S. F. 2014. Association of T-cell co-regulatory protein expression with clinical outcomes following radical cystectomy for urothelial carcinoma of the bladder. *European Journal of Surgical Oncology,* 40**,** 121-7.

ZHANG, P., CHEN, Z., NING, K., JIN, J. & HAN, X. 2017. Inhibition of B7-H3 reverses oxaliplatin resistance in human colorectal cancer cells. *Biochemical and Biophysical Research Communications,* 490**,** 1132-1138.

ZHAO, J., LEI, T., XU, C., LI, H., MA, W., YANG, Y., FAN, S. & LIU, Y. 2013. MicroRNA-187, down-regulated in clear cell renal cell carcinoma and associated with lower survival, inhibits cell growth and migration though targeting B7-H3. *Biochemical and Biophysical Research Communications,* 438**,** 439-444.

ZHAO, X., LI, J., HUANG, S., WAN, X., LUO, H. & WU, D. 2015. MiRNA-29c regulates cell growth and invasion by targeting CDK6 in bladder cancer. *American Journal of Translational Research,* 7**,** 1382-1389.

ZHOU, Z., LUTHER, N., IBRAHIM, G. M., HAWKINS, C., VIBHAKAR, R., HANDLER, M. H. & SOUWEIDANE, M. M. 2013. B7-H3, a potential therapeutic target, is expressed in diffuse intrinsic pontine glioma. *Journal of Neurooncology,* 111**,** 257-64.

8 Publications

Parts of this thesis have contributed to the following publications:

- AICHER, W. K., KORN, M., REITNAUER, L., MAURER, F. B., HENNENLOTTER, J., BLACK, P. C., TODENHOFER, T., BEDKE, J. & STENZL, A. 2021. Expression patterns of the immune checkpoint ligand CD276 in urothelial carcinoma. *BMC Urology,* 21**,** 60. doi: 10.1186/s12894-021-00829-0

Parts of the results of this thesis have been presented at the following conferences:

- F. Maurer, L. Reitnauer, M. Korn, T. Todenhöfer, A., W. K. Aicher (2019) *Exploring the expression of tumor marker CD276/B7-H3 in urothelial carcinoma cell lines and somatic urothelial cells in vitro* (DGU Congress Hamburg 2019)

- M. Korn, F. Maurer, L. Reitnauer, T. Todenhöfer, A. Stenzl, W. K. Aicher (2019*) Expression of CD276 / B7-H3 is significantly elevated in bladder cancer in stages T1 – T4a* (DGU Congress Hamburg 2019)

- W. K. Aicher, F. Maurer, L. Reitnauer, M. Korn, M. Maas, J. Hennenlotter, T. Todenhöfer, A. Stenzl (2020) *Expression of immune checkpoint ligand CD276 (B7-H3) is regulated in urothelial carcinoma on a transcriptional and post-transcriptional level and drops significantly in late-stage tumor tissue samples.* (EAU Convention Amsterdam 2020 poster # 231)

9 Erklärung zum Eigenanteil der Dissertationsschrift

Die Arbeit wurde in der Klinik für Urologie des Universitätsklinikums Tübingen unter Betreuung von Prof. Dr. rer. nat. Wilhelm K. Aicher durchgeführt. Die Konzeption der Studie erfolgte durch ebendiesen. Die Versuche wurden (nach Einarbeitung durch Labormitglieder Fr. Tanja Abruzzese und Fr. Conny Bock) von mir eigenständig durchgeführt. Die Testung der Proben auf eine mögliche *Mycoplasmen*-Kontamination wurde mit Unterstützung von Fr. Tanja Abruzzese durchgeführt. Die Bereitstellung der Proben zur Gewinnung somatischer Referenz-Zellen erfolgte durch die Klinik für Urologie.

Die statistische Auswertung erfolgte nach Beratung durch das Institut für klinische Epidemiologie und Biometrie (namentlich: Lina Maria Serna Higuita) durch mich.

Ich versichere, das Manuskript selbständig verfasst zu haben und keine weiteren als die von mir angegebenen Quellen verwendet zu haben.

Tübingen, den 22.02.2022

10 Acknowledgement

I would like to express my gratitude to Tanja Abruzzese and Conny Bock for their technical training, guidance and excellent technical support and Lina Maria Serna Higuita from the department of clinical epidemiology and applied biometrics for help with the statistical analysis, and Prof. Dr. Wilhelm K. Aicher for his continuous support and assistance in multiple situations.

Furthermore, I would like to thank Jasper Gronowski and Caroline Riedel for their continuous encouragement throughout the whole process of this work.

Finally, I would like to thank all donors of tissue samples for their contribution.